

## AUTHOR'S RESPONSE

Concerning the revision of

*“An improved land biosphere module for use in the DCESS Earth System Model (Version 1.1) with application to the last glacial termination” by Eichinger, R., Shaffer, G., Albarrán, N., Rojas, M., and Lambert, F., 2017, Geoscientific Model Development (gmd-2016-306).*

Dear Dr. David Lawrence,

in consequence of the reviews and the comments on our manuscript, we have performed extensive revisions on the paper. The main points are:

- Former Fig. 1 including its discussion was relocated from the beginning of Sect. 2 to the evaluation section (Sect. 2.4).
- We included the data points in (new) Fig. 1 and a detailed description of how these polynomials were developed.
- We relocated the land biosphere albedo section from the Supplement to the main manuscript. This is a consequence of the new sensitivity studies described below.
- We have expanded the evaluation by an additional simulation with prescribed ice sheet expansion and included the results in Fig. 4 and table 2.
- We have restructured the paper to put the focus squarely on carbon cycle changes driven by the land biosphere and our new developments concerning vegetation and permafrost.
- We have carried out additional sensitivity experiments (nul-vegetation, no permafrost and old albedo, doubled permafrost carbon reservoir) for the assessment of the new developments. These new results are now included in Fig. 5 and partly in Fig. 6 as well as discussed in the text.
- We more clearly state the amount of land carbon inventory and discuss its uncertainties and implications for our results.
- With regard to our reply to the first specific comment of reviewer 1, we decided not to include a specific calculation for methane at this stage. This would have introduced additional complexities and uncertainties and the results would not be relevant to the main conclusions of our paper. Hence, we continued to prescribe atmospheric methane concentrations for the calculation of radiation from data-based reconstructions.
- We now better discuss the conundrum of receiving “worse” results although improving the model, or in other words, getting good results for the wrong reasons.

- We added a number of additional clarifications and explanations and performed all specific suggestions and corrections as announced in our point by point replies to the referees.
- The Supplement has undergone only slight changes: The albedo section is out (now in the main manuscript), and Table S3 as well, the shifted focus of the paper makes the table futile.

Please find below the differences between the last version of the manuscript and the new version as well as our point by point responses to the reviewers.

Best regards,

Roland Eichinger, Gary Shaffer, Nelson Albarrán, Maisa Rojas and Fabrice Lambert

June 21, 2017

# An improved land biosphere module for use in **reduced-complexity** the DCESS Earth System Models-Model (Version 1.1) with application to the last glacial termination

Roland Eichinger<sup>1</sup>, Gary Shaffer<sup>2,3</sup>, Nelson Albarrán<sup>4</sup>, Maisa Rojas<sup>1</sup>, and Fabrice Lambert<sup>5</sup>

<sup>1</sup>Department of Geophysics, University of Chile, Blanco Encalada 2002, Santiago, Chile

<sup>2</sup>GAIA-Antarctica, University of Magellanes, Avenida Bulnes 01855, Punta Arenas, Chile

<sup>3</sup>Niels Bohr Institute, University of Copenhagen, Blegdamsvej 17, Copenhagen, Denmark

<sup>4</sup>Department of Physics, University of Santiago de Chile, Avenida Ecuador 3493, Santiago, Chile

<sup>5</sup>Department of Physical Geography, Catholic University of Chile, Vicuña Mackenna 4860, Santiago, Chile

*Correspondence to:* Roland Eichinger (roland@dgf.uchile.cl)

## Abstract.

Interactions between the land biosphere and the atmosphere play an important role for the Earth's carbon cycle and thus should be considered in studies of global carbon cycling and climate. Simple approaches are a useful first step in this direction but may not be applicable for certain climatic conditions. To improve the ability of the reduced-complexity Danish Center for Earth System Science (DCESS) Earth System Model DCESS to address cold climate conditions, we reformulated the model's land biosphere module by extending it to include three dynamically varying vegetation zones as well as a permafrost component. The vegetation zones are formulated by emulating the behavior of a complex land biosphere model. We show that with the new module, the size and timing of carbon exchanges between atmosphere and land are represented more realistically in cooling and warming experiments. In particular, we use the new module to address carbon cycling and climate change across the last glacial transition. Within the constraints provided by various proxy data records, we tune the DCESS model to a Last Glacial Maximum state and then conduct transient sensitivity experiments across the transition under the application of explicit transition functions for high latitude ocean exchange, atmospheric dust, and the land ice sheet extent. We compare simulated time evolutions of global mean temperature,  $p\text{CO}_2$ , atmospheric and oceanic carbon isotopes as well as ocean dissolved oxygen concentrations with proxy data records. In this way we estimate the importance of different processes across the transition with emphasis on the role of land biosphere variations and find that carbon outgassing from permafrost and uptake of carbon by the land biosphere broadly compensate each other during the temperature rise of the early last deglaciation.

## 1 Introduction

On centennial to millennial time scales, ocean processes may largely determine variations of atmospheric  $\text{CO}_2$  concentrations (Fischer et al., 2010; Sigman et al., 2010). Such processes include changes in ocean dynamics as well as in biogeochemical properties like variations in the phosphate inventory or iron fertilisation (Martin et al., 1990; Maher et al., 2010). However, also interactions between atmosphere and land can have an important impact on the overall change in the carbon cycle and

thus on the Earth's climate system. Net primary production on land takes up  $\text{CO}_2$  from the atmosphere at a rate that increases with the  $p\text{CO}_2$  itself ( $\text{CO}_2$  fertilisation; Saugier et al., 2001). Remineralisation in the soils increases with increasing temperature (Davidson and Janssens, 2006). Different vegetation zones advance and retreat due to varying climate conditions, thereby changing the terrestrial biomass budget and thus the carbon amount being stored in vegetation (Ciais et al., 2012). Moreover, changes in permafrost area and, during glacial conditions, changes in areas covered by ice sheets also have the potential to significantly modify atmospheric  $p\text{CO}_2$  ~~significantly~~ (Schuur et al., 2008). The release of carbon into the atmosphere through the thawing of permafrost in a warming future climate has been assessed in a number of studies (e.g. Schaefer et al., 2011; Schuur et al., 2008; Khvorostyanov et al., 2008) and carbon storage and release in and from permafrost can also help explain glacial-interglacial cycles (Zech, 2012; Ciais et al., 2012; Crichton et al., 2016). A land biosphere module within an Earth System Model should be able to address these processes.

For this reason, we here extend the Danish Center for Earth System Sciences (DCESS) Earth System Model (Shaffer et al., 2008) by a new terrestrial biosphere scheme. ~~This parameterisation~~ Our new module features the three vegetation zones, tropical forests (TF), grasslands-savanna-deserts (GSD) and extratropical forests (~~TFEF~~), through definition of their characteristic values of biomass reservoirs and net primary production (NPP). The dynamic accounting of the latitudinal boundaries of the different zones and thereby their area extents is approximated by fitting polynomial functions of global mean temperature ( $T_{glob}$ ) to results of a complex vegetation model study by Gerber et al. (2004). For completeness we also developed a simple approach to vegetation albedo based on the relative sizes of the three vegetation zones. Moreover, we present a component that accounts for carbon being stored in permafrost and below terrestrial ice sheets to allow extensive carbon storage on land during glacial climate conditions and its release across deglaciation events. In DCESS model simulations, these new developments considerably improve the estimates of amount and timing of land-atmosphere carbon exchanges, including the carbon isotopes  $^{13}\text{C}$  and  $^{14}\text{C}$ .

For a first application of this new module, we furthermore developed a set of explicit functions that describe the transitions of high latitude ocean exchange, atmospheric dust and land ice sheet extent across the last 25 kaBP. This allows us to simultaneously simulate time series of global mean temperature,  $p\text{CO}_2$ , atmospheric and oceanic carbon isotopes as well as ocean dissolved oxygen concentrations across the deglaciation after the Last Glacial Maximum (LGM,  $\sim 21,000$  years ago). Hitherto, the DCESS model has been used mainly for future climate projections (see e.g. Shaffer et al., 2009; Shaffer, 2010) and evaluated for pre-industrial (PI) climate conditions (see Shaffer et al., 2008). For the present application, the model is calibrated to glacial conditions by adapting physical and biogeochemical parameters guided by proxy data records. This includes a physically simple method to generate isolated deep water in the high latitude model ocean (as it had been hypothesised by several studies, e.g. Francois et al., 1997; Sigman and Boyle, 2000; Broecker and Barker, 2007) through the imposition of a depth profile for the vertical exchange intensity. Transient sensitivity simulations across the last 25 kaBP are then performed. These demonstrate the impact and timing of various processes on atmospheric temperatures,  $p\text{CO}_2$  and the carbon isotopes  $^{13}\text{C}$  and  $^{14}\text{C}$  at the beginning of the last glacial termination ("Mystery Interval" (MI), from 17.5 to 14.5 kaBP; Broecker and Barker,

2007) and reveals that carbon outgassing from permafrost and uptake of carbon by the land biosphere broadly compensate each other during the temperature rise of the early last deglaciation.

## 2 A new land biosphere ~~in~~ module for the DCESS model

The DCESS model features components for the atmosphere, ocean, ocean sediment, land biosphere and lithosphere and has been designed for global climate change simulations on time scales from years to millions of years (Shaffer et al., 2008). Its geometry consists of one hemisphere, divided into two 360° wide zones by 52° latitude. The model ocean is divided into a low-mid and a high latitude sector (as in the HILDA (**h**igh-latitude exchange/**i**nterior **d**iffusion **a**dvection) model, developed by Shaffer and Sarmiento, 1995) and features a continuous vertical resolution of 100 m, to a depth of 5500 m. The near surface atmospheric mean temperature is described by a simple, zonal mean, energy balance model in combination with sea ice and snow parameterisations. The atmosphere is assumed to be well mixed for gases and air-sea gas exchange fluxes and transports via weathering, volcanism and interactions with the land biosphere are considered for carbon dioxide (CO<sub>2</sub>) and methane (CH<sub>4</sub>) in <sup>12,13,14</sup>C species, respectively, as well as for nitrous oxide (N<sub>2</sub>O) and oxygen (O<sub>2</sub>). Ocean dynamics are characterised by high latitude sinking and low-mid latitude upwelling as well as horizontal and vertical diffusion between the latitude zones and the ocean layers. For the ocean biogeochemical cycling, a number of tracers are considered (namely, phosphate (PO<sub>4</sub>), dissolved oxygen (O<sub>2</sub>), dissolved inorganic carbon (DI<sup>12,13,14</sup>C), and alkalinity (ALK)), which are forced by new production, air-sea exchange, remineralisation of organic matter, dissolution of CaCO<sub>3</sub>, river inputs and evaporation/precipitation (Shaffer, 1996; Shaffer et al., 2008). There is a sediment section for each of the ocean model layers addressing CaCO<sub>3</sub> dissolution/burial and organic matter remineralisation/burial.

A land biosphere scheme accounts for the <sup>12,13,14</sup>C cycling with leaf, wood, litter and soil boxes (Shaffer et al., 2008). NPP on land takes up CO<sub>2</sub> from the atmosphere and is distributed between leaves and wood. Leaf loss goes to litter, wood loss is divided between litter and soil and litter loss is divided between the atmosphere (as CO<sub>2</sub>) and the soil. Soil loss goes to the atmosphere as CO<sub>2</sub> and CH<sub>4</sub>. Losses from all land reservoirs are taken to be proportional to reservoir size and, for litter and soil, to depend upon the mean atmospheric temperature according to  $\lambda_Q \equiv Q_{10}^{(T_{glob} - T_{glob,PI})/10}$ , where  $Q_{10}$  (a biotic activity increase for a 10 degree increase of  $T_{glob}$ ) is chosen to be 2 (Friedlingstein et al., 2006). ~~With this simplified vegetation scheme, the DCESS model responds to cooling with an increase in land biomass. The terrestrial remineralisation rate decreases with sinking temperatures and hence, more carbon can be stored below ground. However, LGM reconstructions show less carbon in the land biosphere than for warmer, pre-industrial conditions (Peng et al., 1998; Prentice et al., 2011). This simplistic model behaviour can be seen in Fig. 3a, which shows the steady state terrestrial biomass as a function of  $p\text{CO}_2$  and  $T_{glob}$ . These results are generated through prescribing various  $p\text{CO}_2$  and  $T_{glob}$  values in numerous model simulations.~~

Steady state land biomass (GtC) as a function of global mean temperature (°C) and  $p\text{CO}_2$  (ppm) deviations from the calibrated PI value for a) the old uniform biosphere scheme and b) the new biosphere scheme with three vegetation zones. The red circles denote the PI and the blue circles LGM conditions.

When formulated in this simplistic manner, our original biosphere module does not take into consideration changes in vegetated area and thereby overestimates land biosphere biomass for cold conditions (see below). In an attempt to remedy these deficiencies while retaining simplicity on the level of the rest the model, we here present the extension of this scheme to three different vegetation zones. We define a latitudinal distinction of ~~three different~~ these three vegetation zones and their latitudinal boundaries on a global scale. The zones we consider are tropical forests (TF), grasslands, savanna and deserts (GSD) and extratropical forests (EF) containing temperate and boreal forests. In ~~the new version (Fig. 3b), biomass decreases when temperatures sink as vegetation types shift and the snow line moves equatorward (note however that a prescribed ice sheet line is not included in these simulations). The permafrost biomass, however, increases in the course of that process. This shows that the general land carbon storage is represented more realistically in the new model version.~~ In this section, we first present the characteristics of the chosen vegetation zones and their latitudinally variable borders. Then, the new calculations of the biosphere-atmosphere exchange fluxes of CO<sub>2</sub> and CH<sub>4</sub> for <sup>12</sup>C as well as for the rare carbon isotopes <sup>13</sup>C and <sup>14</sup>C are described and a simplified formulation of the treatment of permafrost is given. Moreover, in this section, we provide a brief evaluation of the new vegetation module, to show how it represents land-atmosphere carbon fluxes on centennial to millennial time scales.

## 2.1 Description of the vegetation zones

The three vegetation zones (TF, GSD, ~~BFEF~~) were defined on the basis of a study by Gerber et al. (2004). In that study, the complex LPJ terrestrial biosphere model (Lund-Potsdam-Jena Dynamic Global Vegetation Model) was applied to distinguish between a number of vegetation zones based on several variables. ~~Tab. 1 shows the characteristic values of biomass reservoirs and NPP of those vegetation zones at PI climate conditions for one hemisphere (Gower et al., 1999; Saugier et al., 2001; Sterner and Elser, 2002). The values in Tab. 1 have been constrained such that the sum over the three vegetation zones adds up to PI values of the original biosphere model (Shaffer et al., 2008).~~

~~Tropical Grassland Boreal forest savanna forest desert Leaves / GtC 15 10 25 Wood / GtC 135 90 25 Litter / GtC 8 32 20 Soil / GtC 100 400 250 NPP / Gt a<sup>-1</sup> 12.5 7.5 10~~ Distribution of biomass reservoirs and net primary production of the different vegetation zones at PI conditions, globally averaged for one hemisphere adjusted to the DCESS model geometry (see Chapin et al., 2011, and

The latitudinal limits of these vegetation zones are dynamically defined. In general, the extent of certain vegetation zones depends mainly on temperatures and precipitation. However, the limitations of the DCESS model (no explicit computation of precipitation and restriction to two latitudinal sections) require a somewhat more general approach. We therefore determine the division of the three vegetation zones solely by the deviation of the global mean atmosphere temperature from its PI value (15° C). For this purpose, we derived two polynomial functions from a study by Gerber et al. (2004, in particular from the results in their Fig. 4) Gerber et al. (2004) started from the total tree cover frame of their Fig. 4 by reading off, at 2° C intervals from -10 to 10° C deviation from pre-industrial global mean temperature, the latitudes in the Northern Hemisphere of 50% tree cover both above and below the subtropical zone of lower tree cover. Each of these two sets of 11 points formed the basis of our curve fitting. We found that 5th order polynomials provided good fits to each of these sets. This emulation of a complex vegetation model thereby implicitly includes the role of precipitation in the temperature-dependence of the vegetation zone bound-

aries. The two latitudinal limitations of the vegetation zones are described by the two 5th order polynomials  $L_{TF-GSD}$

$$\underline{L_{TF-GSD}} \approx -1.83 \cdot 10^{-5} \cdot \delta T_{glob}^5 - 0.0005809 \cdot \delta T_{glob}^4 - 0.005168 \cdot \delta T_{glob}^3 + 0.0497 \cdot \delta T_{glob}^2 + 1.092 \cdot \delta T_{glob} + 11.28 \quad (1)$$

$$+ 0.0497 \cdot \delta T_{glob}^2 + 1.092 \cdot \delta T_{glob} + 11.28 \quad (2)$$

and  $L_{GSD-EF} = 1.152 \cdot 10^{-5} \cdot \delta T_{glob}^5 - 0.0001785 \cdot \delta T_{glob}^4 - 0.004557 \cdot \delta T_{glob}^3 + 0.04156 \cdot \delta T_{glob}^2 + 1.017 \cdot \delta T_{glob} + 37.77,$

$$\underline{L_{GSD-EF}} \approx 1.152 \cdot 10^{-5} \cdot \delta T_{glob}^5 - 0.0001785 \cdot \delta T_{glob}^4 - 0.004557 \cdot \delta T_{glob}^3 \quad (3)$$

$$+ 0.04156 \cdot \delta T_{glob}^2 + 1.017 \cdot \delta T_{glob} + 37.77, \quad (4)$$

which depend only on the deviation of the global mean atmosphere temperature  $\delta T_{glob}$  from the calibrated PI steady-state.  $L_{TF-GSD}$  denotes the latitude of the border between the TF and the GSD zones and  $L_{GSD-EF}$  the latitude between GSD and EF. These two 5th order polynomials are illustrated in Fig. 1.

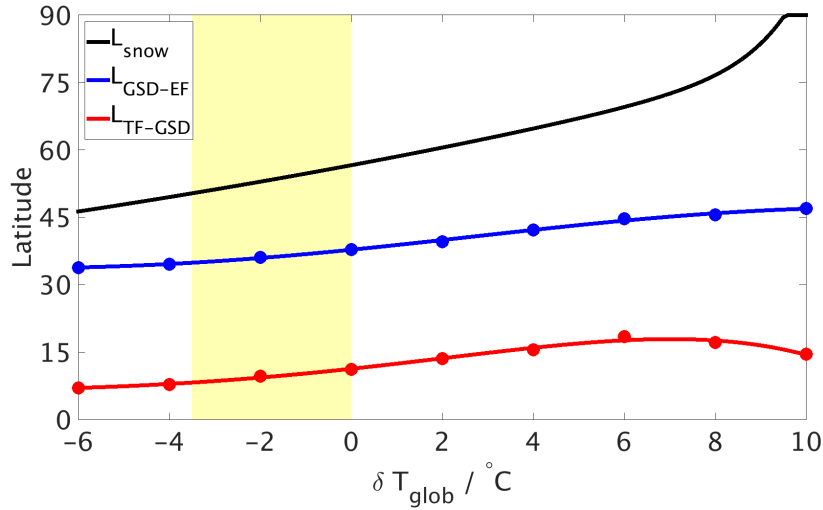


**Figure 1.** Polynomial functions describing the dynamic latitudes of the borders between the three vegetation zones as function of the global mean atmosphere temperature ( $\delta T_{glob}$ ) deviation and the latitude of  $0^\circ\text{C}$ -global-mean-atmosphere-temperature  $L_{snow}$ —the “snowline” (black). Red: Border between the TF and the GSD zone ( $L_{TF-GSD}$ ). Blue: Border between the GSD and the EF zone ( $L_{GSD-EF}$ ). The dots mark the points from the curve fitting as described in the text. The yellow bar marks the region between LGM and PI climate conditions. (PI:  $\delta T_{glob,PI} = 0^\circ\text{C}$ ,  $L_{TF-GSD,PI} = 11.28^\circ$ ,  $L_{GSD-EF,PI} = 37.77^\circ$ ,  $L_{snow,PI} = 55^\circ$ ); LGM: ( $\delta T_{glob,LGM} = -3.5^\circ\text{C}$ ;  $L_{TF-GSD,LGM} = 7.17^\circ$ ;  $L_{GSD-EF,LGM} = 33.92^\circ$ ,  $L_{snow,LGM} = 47^\circ$ — $L_{snow,LGM} = 51^\circ$ )

The EF vegetation zone additionally is limited by either the model “snowline” (defined as the latitude of  $0^\circ\text{C}$ -global-mean temperature)-snowline or the line of the terrestrial ice sheet extent, depending on which one of the two lines expands the farthest

from the pole at the current time step (see Sect. 2.4 for definition of “snowline“ and further explanations). The snowline is also included in Fig. 1, the zone poleward of the snowline is taken to be permafrost area in our simplified approach. Based on these latitudinal limits, the total CO<sub>2</sub> and CH<sub>4</sub> fluxes between the terrestrial biosphere and the atmosphere are now determined by the sum of the three vegetation zones and thereby depend on the areas and mean temperatures of each zone as well as their values of NPP and stored biomass.

Table 1 shows the characteristic values of biomass reservoirs and net primary production (NPP) of those vegetation zones at PI climate conditions ( $T_{glob} = 15^{\circ} C, p_{CO_2} = 280$  ppm) (Gower et al., 1999; Saugier et al., 2001; Sterner and Elser, 2002; Zheng et al., 2008). The values in table 1 have been constrained such that the sum over the three vegetation zones adds up to global PI values of the original biosphere model (Shaffer et al., 2008).

	Tropical forest	Grassland savanna desert	Extratropical forest
Leaves / GtC	30	20	50
Wood / GtC	270	180	50
Litter / GtC	16	64	40
Soil / GtC	200	800	500
NPP / Gt · a <sup>-1</sup>	25	15	20
Area / 10 <sup>6</sup> km <sup>2</sup>	25	53	27

**Table 1.** Pre-industrial distribution of carbon storage among model land carbon pools as well as model net primary production for the three vegetation zones (see Chapin et al., 2011, and citations therein).

10 Furthermore for-

## 2.2 Vegetation albedo

For completeness and consistency, we also extended the model albedo calculation to account for the new biosphere scheme with the three vegetation zones. Non-forest vegetation zones, in our case the GSD zone, have a higher albedo than forest zones, here the TF and the EF zones (Bonan, 2008). Based on the latitudinal approach by Hartmann (1994) that was applied to the DCESS model (Shaffer et al., 2008), we now also take into account In the DCESS model, albedo,  $\alpha$ , is taken to be constant and equal to 0.62 for all snow or ice covered areas. For non-snow/ice covered areas,  $\alpha$  is expressed as

$$\alpha = a + b \cdot \left\{ 0.5 \cdot (3 \cdot \sin\Theta)^2 - 1 \right\} \quad (5)$$

where  $\Theta$  is the latitude,  $b = 0.175$  and  $a = 0.3$  for present day conditions. This functional form and these constant values have been based on present day observations (Hartmann, 1994). The albedo of non-snow/ice covered areas should vary with

vegetation type since forested areas have lower albedo than non-forested areas (Bonan, 2008). As seen in Fig. 1, as the Earth cools from present day, both forested model areas (EF and TF zones) contract while the non-forested model area (GSD zone) expands slightly, in part in response to dryer conditions (Gerber et al., 2004). This would lead to higher albedo and a positive feedback on the cooling. For completeness in our new treatment of the role of the land biosphere in climate and to capture such albedo variations within the context of our new land biosphere module, we assume that  $a$  in Eq. 5 may be related to vegetation type such that

$$a = 0.3 - \gamma \cdot \left( 1 - \frac{frac(\delta T_{glob})}{frac_0} \right) \quad (6)$$

where the factor 0.3 is the present day value of  $a$ ,  $\gamma$  is a multiplier, the value of which is determined by calibration (see below),  $frac$  is the ratio of the GSD-vegetation-area of the GSD zone to the overall-vegetation-area-total non-snow/ice covered area (i.e. the sum of the areas of the EF, GSD and TF zones) and  $frac_0$  is this ratio for present day. Note that  $frac(\delta T_{glob})$  can be taken from Fig. 1 or calculated explicitly using Eqs. 5 and 6 and the snowline/ice sheet dependency on  $\delta T_{glob}$  (see Fig. S3 in the Supplement). Fig. 2a shows a plot of  $frac(\delta T_{glob})/frac_0$ .

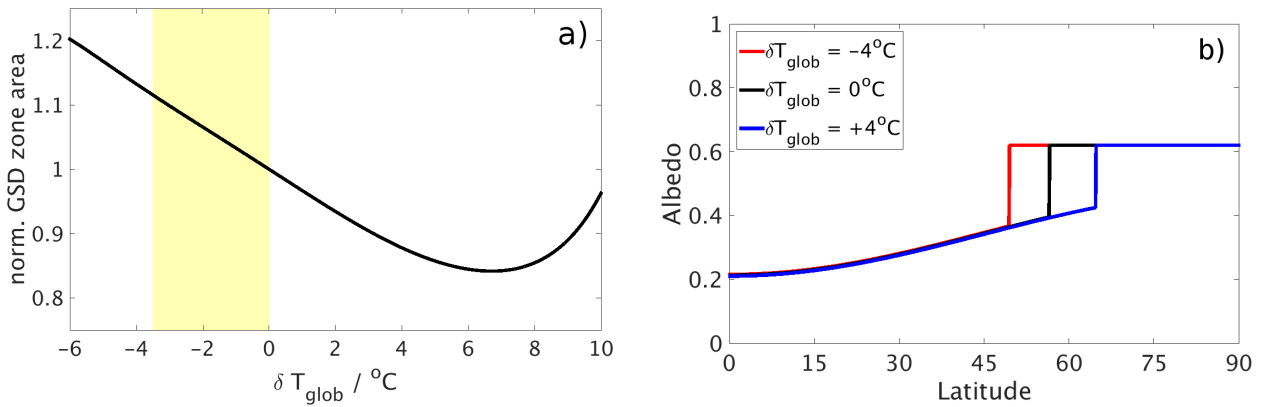


**Figure 2.** a) Normalised GSD zone area fraction as function of global mean temperature deviation from PI climate conditions. The yellow bar marks the region between LGM and PI. b) Latitude dependency of albedo for three different deviations from the global mean temperature ( $-4^\circ\text{C}$ ,  $0^\circ\text{C}$  and  $4^\circ\text{C}$ ). Note that poleward of the snow line the albedo is 0.62 (albedo of snow/ice covered area).

The vegetation albedo forcing for the albedo calculation. For this, the model was calibrated to give a vegetation albedo radiative forcing anomaly of about for LGM conditions. Such details are found in the supplementary material. the LGM ( $\delta T_{glob} = -3.5^\circ\text{C}$ ) relative to present day has been determined in more complex models from which we choose the value of  $-0.7\text{ W/m}^2$  as being representative (Köhler et al., 2010). Together with Eq. 6 and the model latitudinal distribution of solar forcing, we find that this LGM vegetation albedo forcing anomaly is obtained in our model simulation for a  $\gamma$  value of 0.02, a value we adopt here. Fig. 2b illustrates new albedo distributions with latitude for the specific cases of  $\delta T_{glob} = -4$ , 0 and  $4^\circ\text{C}$  for which  $a = 0.3027$ , 0.3 and 0.2976, respectively.

### 2.3 Extension of the carbon flux equations

In the original version of the DCESS terrestrial biosphere module (Shaffer et al., 2008), the global vegetation NPP is determined by

$$NPP = NPP_{PI} \left( 1 + f_{CO_2} \cdot \ln \left( \frac{pCO_2}{pCO_{2,PI}} \right) \right). \quad (7)$$

5 Now, we subdivide this equation into three equations

$$NPP_{TF} = NPP_{TF,PI} \cdot A_{TF} \cdot \left( 1 + f_{CO_2} \cdot \ln \left( \frac{pCO_2}{pCO_{2,PI}} \right) \right), \quad (8)$$

$$NPP_{GSD} = NPP_{GSD,PI} \cdot A_{GSD} \cdot \left( 1 + f_{CO_2} \cdot \ln \left( \frac{pCO_2}{pCO_{2,PI}} \right) \right) \quad (9)$$

and

$$10 \quad NPP_{EF} = NPP_{EF,PI} \cdot A_{EF} \cdot \left( 1 + f_{CO_2} \cdot \ln \left( \frac{pCO_2}{pCO_{2,PI}} \right) \right) \quad (10)$$

for the different vegetation zones, respectively. Thus, the global NPP is now determined by the sum of the NPP of the three vegetation zones:

$$NPP = NPP_{TF} + NPP_{GSD} + NPP_{EF} \quad (11)$$

The factors  $A_{TF}$ ,  $A_{GSD}$  and  $A_{EF}$  are calculated by

$$15 \quad A_{TF} = \frac{\sin(L_{TF-GSD})}{\sin(L_{TF-GSD,PI})}, \quad (12)$$

$$A_{GSD} = \frac{\sin(L_{GSD-EF} - L_{TF-GSD})}{\sin(L_{GSD-EF,PI} - L_{TF-GSD,PI})} \quad (13)$$

and

$$A_{EF} = \frac{\sin(L_s) - \sin(L_{GSD-EF})}{\sin(L_{s,PI}) - \sin(L_{GSD-EF,PI})} \quad (14)$$

20 and scale the contributions of the respective NPP by the current area of the individual vegetation zone. The index  $PI$  stands for reference PI conditions and  $f_{CO_2}$  for the  $CO_2$  fertilisation factor. In the original configuration, this factor was set to 0.65, which was in good agreement with results by Friedlingstein et al. (2006). However, a revision of this value in a model intercomparison study yielded a lower value of 0.37 to be a more suitable value for the terrestrial biosphere (Zickfeld et al., 2013) (Zickfeld et al., 2013; Eby  
25 2008) is now calculated separately for the three vegetation zones as well.

Now, the four conservation equations per carbon isotope (<sup>12,13,14</sup>C) (see Shaffer et al., 2008) have to be calculated for each vegetation zone separately. The losses for reservoir size of litter and soil were dependent on the mean global atmosphere temperature in Shaffer et al. (2008) for the uniform vegetation. In order to achieve a more realistic dependency of this process in the three vegetation zone scheme, we now approximate a mean atmosphere temperature for each vegetation zone separately by making use of the DCESS model latitudinal temperature profile expressed as a second order Legendre polynomial in sine of latitude (Shaffer et al., 2008). This yields,

$$T_{TF} = \frac{(T_{atm,LL} - 0.5 \cdot T_{atm,HL}) \cdot \sin(L_{TF-GSD}) + 0.5 \cdot T_{atm,HL} \cdot \sin(L_{TF-GSD})^3}{\sin(L_{TF-GSD})}, \quad (15)$$

~~$$T_{GSD} = \frac{(T_{atm,LL} - 0.5 \cdot T_{atm,HL}) \cdot (\sin(L_{GSD-EF}) - \sin(L_{TF-GSD})) + 0.5 \cdot T_{atm,HL} \cdot (\sin(L_{GSD-EF})^3 - \sin(L_{TF-GSD})^3)}{\sin(L_{GSD-EF}) - \sin(L_{TF-GSD})} \text{ and } T_{EF} = \frac{(T_{atm,LL} - 0.5 \cdot T_{atm,HL}) \cdot (\sin(L_{snow/ice}) - \sin(L_{TF-GSD})) + 0.5 \cdot T_{atm,HL} \cdot (\sin(L_{snow/ice})^3 - \sin(L_{TF-GSD})^3)}{\sin(L_{snow/ice}) - \sin(L_{TF-GSD})}$$~~

$$\underline{T_{GSD}} \equiv \frac{(T_{atm,LL} - 0.5 \cdot T_{atm,HL}) \cdot (\sin(L_{GSD-EF}) - \sin(L_{TF-GSD}))}{\sin(L_{GSD-EF}) - \sin(L_{TF-GSD})} \quad (16)$$

$$+ \frac{0.5 \cdot T_{atm,HL} \cdot (\sin(L_{GSD-EF})^3 - \sin(L_{TF-GSD})^3)}{\sin(L_{GSD-EF}) - \sin(L_{TF-GSD})} \quad (17)$$

and

$$\underline{T_{EF}} \equiv \frac{(T_{atm,LL} - 0.5 \cdot T_{atm,HL}) \cdot (\sin(L_{snow/ice}) - \sin(L_{TF-GSD}))}{\sin(L_{snow/ice}) - \sin(L_{TF-GSD})} \quad (18)$$

$$+ \frac{0.5 \cdot T_{atm,HL} \cdot (\sin(L_{snow/ice})^3 - \sin(L_{TF-GSD})^3)}{\sin(L_{snow/ice}) - \sin(L_{TF-GSD})}. \quad (19)$$

Here,  $T_{atm,LL}$  denotes the mean atmosphere temperature in the DCESS model low-mid latitude sector ( $0^\circ - 52^\circ$ ) and  $T_{atm,HL}$  in the model high latitude sector ( $52^\circ - 90^\circ$ ).  $L_{snow/ice}$  stands for the minimum of the latitude of the snow and the ice sheet line (see next section). Now,  $\lambda_Q$ , which influences the decay of litter and soil, can be calculated for each vegetation zone separately with  $\lambda_Q^i \equiv Q_{10}^{(T^i - T_{PI}^i)/10}$ , where the index  $i = 1, 2, 3$  stands for the three vegetation zones TF, GSD and EF. The conservation equations for the land biosphere reservoirs of <sup>12</sup>C from Shaffer et al. (2008) for leaves ( $M_G$ ), wood ( $M_W$ ), litter ( $M_D$ ) and soil ( $M_S$ ) thus split into twelve equations, four for each vegetation zone:

$$\frac{dM_G^i}{dt} = \frac{35}{60} \cdot NPP^i - \frac{35}{60} \cdot NPP_{PI}^i \cdot \frac{M_G^i}{M_{G,PI}^i} \quad (20)$$

15

$$\frac{dM_W^i}{dt} = \frac{25}{60} \cdot NPP^i - \frac{25}{60} \cdot NPP_{PI}^i \cdot \frac{M_W^i}{M_{W,PI}^i} \quad (21)$$

$$\frac{dM_D^i}{dt} = \frac{25}{60} \cdot \frac{35}{60} \cdot NPP^i \cdot \frac{M_G^i}{M_{G,PI}^i} + \frac{20}{60} \cdot NPP_{PI}^i \cdot \frac{M_W^i}{M_{W,PI}^i} - \frac{55}{60} \cdot NPP_{PI}^i \cdot \lambda_Q^i \cdot \frac{M_D^i}{M_{D,PI}^i} \quad (22)$$

$$\frac{dM_S^i}{dt} = \frac{5}{60} \cdot NPP^i \frac{M_W^i}{M_{W,PI}^i} + \frac{10}{60} \cdot NPP_{PI}^i \cdot \lambda_Q^i \cdot \frac{M_D^i}{M_{D,PI}^i} - \frac{15}{60} \cdot NPP_{PI}^i \cdot \lambda_Q^i \cdot \frac{M_S^i}{M_{S,PI}^i} \quad (23)$$

Analogously, these equations are extended for the rare carbon isotopes  $^{13}\text{C}$  and  $^{14}\text{C}$ , where fractionation factors for land photosynthesis and, for  $^{14}\text{C}$ , radioactive sinks are considered (Shaffer et al., 2008). The flux of carbon dioxide between the terrestrial biosphere and the atmosphere is then determined by

$$F_{CO_2} = \sum_{i=1}^3 -NPP^i + \frac{45}{55} \cdot \frac{dM_D^i}{dt} \cdot \frac{M_D^i}{M_{D,PI}^i} \cdot NPP_{PI}^i \cdot \lambda_Q^i + \frac{dM_S^i}{dt} \cdot \frac{15}{60} \cdot NPP_{PI}^i \cdot \lambda_Q^i \cdot \frac{M_S^i}{M_{S,PI}^i} \quad (24)$$

As indicated above,  $M_D^i$  and  $M_S^i$  represent the biomass carbon reservoirs in litter and soil for the different vegetation zones, respectively, and  $dM_D^i/dt$  and  $dM_S^i/dt$  their decay rates. For the two rare carbon isotopes, additionally the corresponding fractionation factors  $^{13,14}\alpha$  have to be considered. The flux is then given by

$$F_{^{13,14}CO_2} = \sum_{i=1}^3 -NPP^i \cdot \frac{^{13,14}C}{^{12}C} \cdot ^{13,14}\alpha + \frac{45}{55} \cdot \frac{dM_D^i}{dt} \cdot \frac{^{13,14}M_D^i}{^{13,14}M_{D,PI}^i} \cdot NPP_{PI}^i \cdot \lambda_Q^i \cdot \frac{^{13,14}M_D^i}{^{13,14}M_{D,PI}^i} + \frac{dM_S^i}{dt} \cdot \frac{15}{55} \cdot \frac{^{13,14}M_S^i}{^{13,14}M_{S,PI}^i} \cdot NPP_{PI}^i \cdot \lambda_Q^i \cdot \frac{^{13,14}M_S^i}{^{13,14}M_{S,PI}^i} \quad (25)$$

10

## 2.4 Formulation of permafrost

On glacial-interglacial time scales, global temperature changes lead to terrestrial ice sheet advances and retreats. These can cover large parts of the terrestrial biosphere and thereby prevent land-atmosphere carbon exchange in these areas. In the DCESS model, we account for this by introducing the parameter  $L_{ice}$ , that limits the poleward extent of the **BF-EF** vegetation zone. During interglacials, when ice sheets retreat poleward to about  $70^\circ$  latitude, ~~this limitation is determined by the the poleward boundary of this zone is taken to be the equatorward~~ extent of permafrost, ~~characterised by the parameter  $L_{snow}$  that is defined as the latitude of~~. For simplicity, we assume this extent to be the latitude of our model equatorward snow cover extent,  $L_{snow}$ , defined by the latitude at which global mean atmospheric temperature is  $0^\circ\text{C}$  global mean temperature.  $C$  in our zonally-averaged model. Hence, the minimum of these two parameters ( $L_{snow,ice} = \min(L_{snow}, L_{ice})$ ) at the current time step is used to determine the limitation of the **BF-EF** vegetation zone. When  $L_{snow/ice}$  advances and retreats on large spatial scales, organic carbon is buried/released below/from permafrost areas or areas below terrestrial ice sheets. That means that, additional land-atmosphere carbon ( $^{12,13,14}\text{C}$ ) flux variations due to the changes of permafrost/ice sheet area are considered. For this, we add the permafrost flux term  $^{12,13,14}F_{CO_2,PF}$  to Eqs. 24 and 25, which is calculated by

$$^{12,13,14}F_{CO_2,PF} = \frac{dA_{snow/ice}}{dt} \cdot ^{12,13,14}C_{PF} \quad (26)$$

25

$$\frac{dA_{snow/ice}}{dt} = 2\pi R \cdot \left[ \left(1 - \frac{270}{360}\right) \cdot \left( (1 - \sin(L_{snow/ice}^t)) - (1 - \sin(L_{snow/ice}^{t-1})) \right) \right] \quad (27)$$

and denotes the change in snow or ice covered area. For this,  $L_{snow/ice}$  of the previous ( $t - 1$ ) and the current ( $t$ ) time step is taken.  $R$  denotes the Earth radius and the factor  $(1 - 270/360)$  takes account for the land fraction in the model geometry.

$^{12}C_{PF}$ , the amount of carbon being stored in permafrost, was approximated to  $30 \text{ kg} \cdot \text{m}^{-2}$  by Schuur et al. (2015).

Mainly due to the spatial heterogeneity of permafrost area and organic carbon content in permafrost soils, for example some peatland areas contain more than  $100 \text{ kg} \cdot \text{m}^{-2}$ , others far less than  $30 \text{ kg} \cdot \text{m}^{-2}$ , this value bears large uncertainties (see e.g. Zimov et al., 2009; Crichton et al., 2014). In a sensitivity experiment, we therefore also apply a doubled permafrost carbon content. As shown in Zimov et al. (2009), carbon release rates from permafrost for warming are rapid with time scales on the order of 100 years. Such time scales are comparable to those of extra-terrestrial forest reoccupation of areas freed from permafrost, a process that we also take to be "instantaneous" in the model. On the other hand, carbon buildup in permafrost during cooling is a much slower process (Zimov et al., 2009). However, the model application in the present study starts from LGM conditions, following 80,000 years of cooling. Thus, we feel that this very simplified permafrost approach should be able to capture the first order effects of permafrost on carbon cycling during deglaciation. In fact, when we reduce atmospheric temperatures, the new vegetation scheme reacts with a vegetation decrease (in opposite to the old scheme) and thereby a  $p \text{ CO}_2$  increase, which again increases temperatures. Despite its simplicity, the permafrost implementation therefore helps to generate glacial conditions through its land carbon storage.

For the stable  $^{13}C_{PF}$  isotope, carbon is buried and released through permafrost with the same isotope ratio. We hence set the value to  $\delta^{13}C = -24\text{‰}$  (Zech (2012) estimates this value to  $-27\text{‰}$ ). Using Eq. S9 of the Supplement, this yields a value of  $0.33 \text{ kg} \cdot \text{m}^{-2}$  for permafrost  $^{13}C$  given the above described assumption of permafrost  $^{12}C = 30 \text{ kg} \cdot \text{m}^{-2}$ . For the doubled permafrost carbon experiment, this simply results in a doubled  $^{13}C$  permafrost content. For  $^{14}C_{PF}$ , however, radioactive decay ( $T_{1/2}(^{14}C) \approx 5730 \text{ a}$ ) across glacial periods, when large parts of the high latitudes are covered by terrestrial ice sheets, has to be considered. While being buried with the current isotope ratio of soil, we therefore assume carbon to be released from permafrost radiocarbon free ( $\Delta^{14}C = -1000\text{‰}$ ). This has also been considered to be reasonable by Zech (2012) for the last deglaciation. As is, the land area of the model simply covers 1/4 Land area uniformly covers 25% of the globe from the equator to 70 degrees latitude. In our configuration for the in the one hemisphere, DCESS model. For our model last glacial termination, permafrost affects latitudes between  $47^\circ$  and around  $54^\circ$  (see Fig. S3 in the Supplement) and Sect. 3.1 for explanations, and is estimated as a two hemisphere mean. Across these latitudes, the land fraction averaged over both hemispheres is around 30% (see e.g. Matney, 2012). Thus, a further adjustment for we did not deem necessary to further scale the permafrost effect due to land fraction was not considered to be necessary global mean land fraction.

## 2.5 Evaluation of the new module

As a test of to what extent the newly developed land biosphere scheme adequately represents the behaviour of the different vegetation zones land biosphere for global climate changes, we now present a more some detailed evaluation of a cooling simulation. For this purpose the new module. With the old, simplified vegetation scheme, the DCESS model responds to cooling with an increase in land biomass. The terrestrial remineralisation rate decreases with sinking temperatures and hence,

more carbon can be stored below ground. However, LGM reconstructions show less carbon in the land biosphere than for warmer, pre-industrial conditions (Peng et al., 1998; Prentice et al., 2011). This simplistic model behaviour can be seen in Fig. 3a, which shows the steady state terrestrial biomass as a function of  $p\text{CO}_2$  and  $T_{glob}$ . These results are generated through prescribing various  $p\text{CO}_2$  and  $T_{glob}$  values in numerous 2 ka model simulations. In the new version (Fig. 3b),

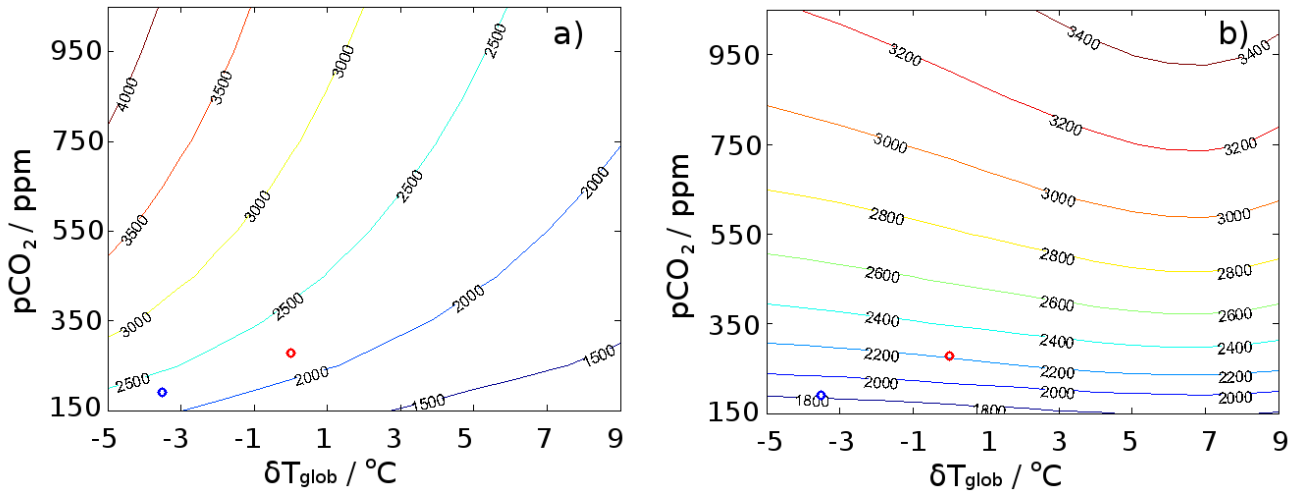


**Figure 3.** Steady state land biomass (GtC) as a function of global mean temperature ( $^{\circ}\text{C}$ ) and  $p\text{CO}_2$  (ppm) deviations from the calibrated PI value for a) the old uniform biosphere scheme and b) the new biosphere scheme with three vegetation zones. The red circles denote PI and the blue circles LGM conditions.

- biomass decreases when temperatures sink as vegetation types shift and the snow line moves equatorward (note however that a prescribed ice sheet line is not included in these simulations). The permafrost biomass, however, increases in the course of that process (not shown). The results in Fig. 3 show that the general land carbon storage is represented more realistically in the new model version.

Futhermore, we show the response of the model vegetation zones and the different vegetation reservoirs to a reduction of atmospheric temperatures and  $p\text{CO}_2$  to LGM conditions. ~~Moreover, we and~~ compare the results with complex vegetation models as well as with data reconstructions.

To evaluate the vegetation scheme for LGM conditions, we carried out cooling simulations with the new and with the old biosphere scheme. For these, we started from a PI steady-state ( $T_{glob} = 15^{\circ}\text{C}$ ,  $p\text{CO}_2 = 280$  ppm), but prescribed the global mean temperature to  $T_{glob} = 11.5^{\circ}\text{C}$  (see Shakun et al., 2012) and the atmospheric  $p\text{CO}_2$  concentration to 190 ppm (e.g. Monnin et al., 2001). A third cooling simulation was conducted with the new biosphere scheme and conditions as described but with an additional prescription of the ice sheet line to  $47^{\circ}$  latitude (see Sect. 3.1). Fig. 4a shows the global sum of total land biomass (LB) carbon for the two (without carbon stored in permafrost) for the three cooling simulations as well as LB carbon for the three individual vegetation zones and Fig. 4b shows LB carbon of the vegetation reservoirs above ground (leaves + wood)

and below ground (litter + soil) for the ~~two simulations~~. ~~Since the system seems to be in equilibrium after around~~, we ~~three~~ ~~simulations~~. We integrated these simulations over 2 ka ~~to reach equilibrium~~.

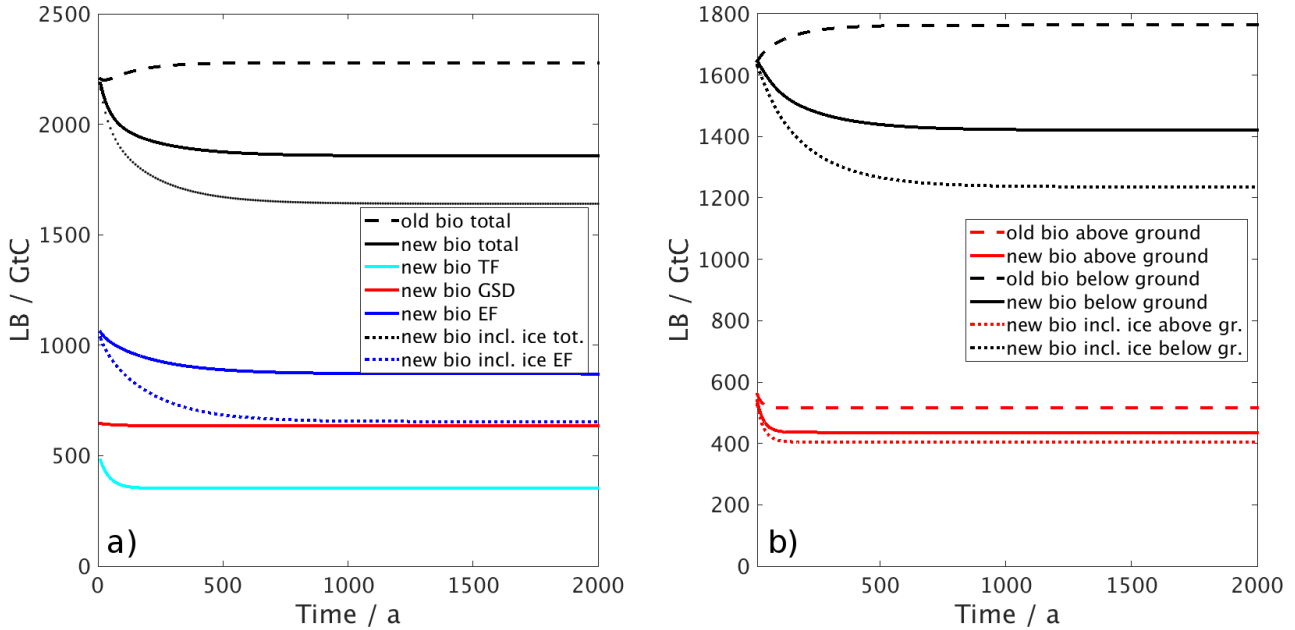


**Figure 4.** Cooling simulation (see text) for the model version with the ~~old~~ (dashed lines) and the new ~~vegetation scheme without~~ (solid lines) and ~~the old with prescribed ice sheet expansion~~ (dasheddotted lines) ~~vegetation scheme~~. a) Total land biomass carbon (in black) and separated into the three vegetation zones (TF: cyan, GSD: red, EF: blue) for the new vegetation scheme. b) Land biomass carbon separated into the reservoirs above ground (leaves + wood) in red and below ground (litter + soil) in black.

As already presented in Fig. 3, the cooling experiment again demonstrates that LB carbon increases in the old model version and decreases with the new biosphere scheme. Fig. 4b shows that the unrealistic increase of LB carbon is ~~mainly~~ due to an increase in litter/soil carbon (~~i.e. biosphere below ground~~). In the simulation with the new biosphere scheme, this does not happen, ~~mainly because of~~. ~~The EF zone is dominated by biosphere below ground and due to~~ the limitation of the poleward expansion of the EF zone through the snow line, ~~this carbon reservoir is now decreasing~~. Also, the figures show that the timing of the change is represented more nuanced with the new biosphere scheme. The biospheres in the three vegetation zones show different reaction times according to their distinct temperatures and the dominating pool of vegetation in the respective area. ~~When we also include the expansion of ice sheets ( $L_{ice} = 47^\circ$ , for explanation see Sec. 3.1), covering larger areas of the EF vegetation zone than the snow line, the total land carbon pool decrease is stronger (dotted lines). It is mainly the biosphere below ground, exclusively in the EF zone, that accounts for this.~~

A poleward limitation of the biosphere in the old ~~vegetation~~ scheme also leads to a reduction of LB carbon in the cooling simulation. To ~~confirm-test~~ this, we performed an additional simulation with the old vegetation scheme, but with ~~a-the~~ crude vegetation area limiting approach  $A = (\sin(L_{snow})/\sin(L_{snow,PI}))^2$ . In this cooling experiment, ~~the total LB carbon~~

decreases, but not as much as with the new biosphere [scheme](#) and the decrease happens faster than with the new biosphere scheme (not shown). The LB change in the EF zone mainly depends on variations in soil, which has a slow response time and is the largest biomass reservoir (Fig. 4a). The TF zone adapts much quicker to the new climate conditions because in this vegetation type the biomass is dominated by leaves and wood. [This shows that not only the quantitative, but also the temporal description of land biomass changes is represented more accurately now.](#) The GSD vegetation zone shows the smallest change in biomass, because in the cooling ~~simulation~~ [simulations](#) the area of this vegetation zone changes only slightly, but rather just shifts latitudinally.

We calibrated the latitudinal dependency of the vegetation zone borders to match the LPJ model results. However, the calculation of carbon stored in the terrestrial biosphere at different climate conditions also depends on other parameters. Hence, we also evaluate the performance of the new DCESS vegetation scheme by comparing it to the results of the LPJ model study by Gerber et al. (2004). For this, [Tab. table 2](#) shows the percentual change of biomass carbon in the cooling experiment ~~with the new and the old DCESS model version, as well as for the new vegetation scheme with and without ice sheet prescription and for the old version with vegetation scheme with and without the biosphere area limit (old bio plus) and as well as for the LPJ model.~~

$\Delta$ LB / %	Total	Litter + Soil	Leaves + Wood
Old bio	+3.0	+9.5	-14.5
Old bio plus	-10.8	-5.2	-26.0
New bio	-18.0	-14.2	-28.5
<a href="#">New bio ice</a>	<a href="#">-27.6</a>	<a href="#">-25.3</a>	<a href="#">-33.6</a>
LPJ	-24.8	-24.7	-25.0

**Table 2.** Percentual change of biomass carbon in the cooling experiment for total biomass and divided into reservoirs above and below ground. DCESS model with [the old biosphere scheme, with and without the crude approach for vegetation area limiting \(see text\)](#), and with [the new biosphere scheme with and without prescribed ice sheet expansion](#), and LPJ model study presented in Gerber et al. (2004).

This comparison demonstrates that in relation to the LPJ model, the adaptation of the LB to different climate conditions is captured much better with the new biosphere scheme. While with the old model version, biomass carbon increased, the new biosphere scheme produces most of the change that the LPJ model shows. Most of the improvement in LB variations through the new vegetation scheme is due to the snow line, that limits the poleward expansion of the biosphere. Using the old biosphere with additional vegetation area limitation, LB carbon decreases under LGM climate conditions. However, with the new vegetation scheme, the snow line particularly limits the EF zone ~~, which is dominated by litter and soil~~ and this largely improves the overall representation of biomass below ground. When vegetation area reduction ~~was is~~ applied to the old biosphere module, the biomass change above ground was already in good agreement with the LPJ model. Hence, the reason for the much larger changes in overall biomass between the old and the new model version as shown in Fig. 4 is mainly due to the better represen-

tation of the slow change of the soil biomass in the EF zone. This more accurate representation of soil in the EF zone, however, is also due to the fact that now the biomass reservoir of each vegetation zone depends on the specific temperature of the zone in question and not on the global mean temperature as in the old model version. The prescribed ice sheet line at 47° latitude generates a further drawdown of the land carbon stock. The percentual change is then close to the LPJ model, about 3% higher.

5 Vegetation above ground changes too much, although this type of vegetation is not affected much by the ice line (see Fig. 4b), but due to the low total amount, the percentual change is high.

Peng et al. (1998) provide an overview of various studies that estimate the reduction in global land biomass for the LGM compared to present day. Those are based on either global climate model simulations, marine carbon isotope data changes or  
10 vegetation mapping approaches. Altogether, these studies show a large spread from 0 (Prentice and Fung, 1990) to  $-1350 \text{ GtC}$  (Adams et al., 1990). The majority of the studies show values between  $-300$  and  $-700 \text{ GtC}$ , a more recent modelling study by Prentice et al. (2011) provides values of  $-550$  to  $-694 \text{ GtC}$ . Through the implementation of the new vegetation scheme, the DCESS model biomass carbon change between PI and LGM does improve from  $+43$  to  $-408 \text{ GtC}$ . ~~Thus results with the new model version agree well other estimates, albeit at their low end~~ Indeed when this calculation includes the effect of ice sheet  
15 extent to 47°, the LGM biomass change is  $-626 \text{ GtC}$ , in excellent agreement with the estimates cited above. Carbon stored in permafrost is around  $600 \text{ Gt}$  for PI conditions and around  $1000 \text{ Gt}$  for LGM climate when the ice sheets are included. Hence, the total amount of carbon on land is about  $2800 \text{ Gt}$  for PI and  $2600 \text{ Gt}$  for the LGM. Ciais et al. (2012) estimate the LGM global carbon stock to  $3640 \pm 400 \text{ Gt}$ , so somewhat higher than in our model. Parts of this is due to our estimation of  $30 \text{ GtC} \cdot \text{m}^{-2}$  for permafrost from Schuur et al. (2015). This apparent underestimation of the permfrost carbon inventory has  
20 to be kept in mind when analysing the model results and it will be addressed in the following with a sensitivity experiment using  $60 \text{ GtC} \cdot \text{m}^{-2}$  for permafrost, for which the total amount of LGM carbon on land will be about  $3600 \text{ Gt}$ .

Overall, it can be stated that the new biosphere scheme with the three vegetation zones constitutes a significant improvement for the representation of the terrestrial biomass as well as the estimates of the size and timing of carbon exchanges between the terrestrial biosphere and the atmosphere. This new implementation better captures the complex interactions between the  
25 terrestrial and the atmospheric carbon exchange as is required for a better understanding of the processes that determine climate changes on glacial-interglacial time scales.

### 3 Application to Last Glacial Maximum and deglaciation

As a first application of the new DCESS terrestrial biosphere module, we simulate the deglaciation after the LGM, when global atmospheric temperatures rose by around  $3.5 \text{ K}$  (Shakun et al., 2012) and atmospheric  $p\text{CO}_2$  increased from  $190 \text{ ppm}$  during the  
30 LGM to Holocene conditions of  $260 \text{ ppm}$  in a series of steps (e.g. Monnin et al., 2001). The most marked of these steps is a steep  $38 \text{ ppm}$  rise near the onset of the deglaciation, the Mystery Interval (Broecker and Barker, 2007). In the Supplement, we provide a literature review with details about the Mystery Interval including current hypotheses for the explanation of that climate change. Earlier studies found considerably greater LGM global mean cooling (Schneider von Deimling et al., 2006); recent

[estimates based on much improved temperature data, however, have shown LGM cooling of 3.2 – 4 K \(Schmittner et al., 2011; Shakun et al., 2012\)](#)

A complete explanation for the  $p\text{CO}_2$  and temperature increase at the onset of the last glacial termination must be able to reproduce a simultaneous decrease by 0.3‰ and 160‰ of atmospheric  $\delta^{13}\text{C}$  (Schmitt et al., 2012) and  $\Delta^{14}\text{C}$  (Reimer et al., 2013), respectively. Furthermore, it should also include how LGM deep water with high salinity (Adkins et al., 2002), low  $\delta^{13}\text{C}$  (Curry and Oppo, 2005) and  $\Delta^{14}\text{C}$  (Burke and Robinson, 2012) and low dissolved oxygen concentrations (but not widespread anoxia) (Jaccard et al., 2014) was formed during the last glacial. Hence, it requires the consideration of a globally comprehensive picture of the physical and biogeochemical processes in atmosphere, ocean and on land, as well as their interactions on various time scales. With its new biosphere scheme, the DCESS model is now better suited for investigations of that kind. However, a number of further adaptations need to be made to simulate LGM conditions and the transition to the Holocene. These are presented next followed by transient simulations across the last 25 kaBP. For these, the model was initialised and forced with the conditions described in Sect. 3.1. Since we focus on the MI (17.5 – 14.5 kaBP), we mainly present and discuss the time period from 20 to 10 kaBP. We assess the impact of various processes on the overall climate change with a focus on the new biosphere scheme and permafrost. In the process, we also evaluate proposed time series for the production of  $^{14}\text{C}$  in the atmosphere.

### 3.1 Model Last Glacial Maximum and transition

Guided by proxy-data records, we first modified several biogeochemical and physical parameters to generate a model steady-state that represents the LGM well. For this, a number of parameters can be considered as possible candidates (see e.g. Kohfeld and Ridgwell, 2009). However, under consideration of the possibilities provided by the enhanced model and knowledge about candidate parameters, we decided upon the adaptations described below.

Increased iron supply and thereby ocean fertilisation (Martin et al., 1990) through enhanced atmospheric dust concentrations during the LGM (see e.g., Mahowald et al., 1999, 2006b; Maher et al., 2010), particularly in the high southern latitudes (e.g. Lambert et al., 2013, 2015), probably led to enhanced new production of organic matter in the Southern Ocean (SO) by way of iron fertilization (see also Lamy et al., 2014; Martínez-García et al., 2014). To account for this, we modified the efficiency factor for new production in the model high latitude ocean sector from 0.36 (standard value for PI conditions, see Shaffer et al., 2008) to 0.5. This leads to a reasonable productivity increase of around 40% for the area of the SO and induces an atmospheric  $p\text{CO}_2$  reduction of around 20 ppm, consistent with the DCESS model iron fertilisation results in Lambert et al. (2015). Moreover, an additional radiative effect of  $-1 \text{ W m}^{-2}$  (Mahowald et al., 2006a) for glacial conditions through atmospheric dust during the LGM is considered. For the transient simulations from the LGM to the Holocene, we have developed a transfer function between temperature and dust fluxes from proxy data records that we applied to the efficiency factor and to the radiative effect. It yielded an exponential dependency of dust with temperature; details can be found in the Supplement.

The lower sea level during the LGM (around 130 m, see e.g., Waelbroeck et al., 2002; Lambeck et al., 2014) and a thereby reduced ocean volume by around 3.5% (see e.g. Adkins and Schrag, 2002) is accounted for by increasing phos-

phate concentrations (the nutrient limiting source in the DCESS ocean biochemistry) and the ocean salinity (see Adkins et al., 2002) by 3.5%. For the transition of these parameters across the last 25 kaBP, we use the latest sea level reconstruction time series from Lambeck et al. (2014). We do not account for the expansion of land mass and vegetation due to reduction of sea level, which causes additional carbon storage (Joos et al., 2004). Although Joos et al. (2004) found that this effect is less important than the effect through climate/CO<sub>2</sub> caused vegetation changes or the ice sheet area effect, it can still have a considerable impact in deglaciation simulations and should be kept in mind when evaluating results. To generate LGM conditions for  $\Delta^{14}\text{C}$  in atmosphere and ocean, we applied the average cosmogenic  $^{14}\text{C}$  production rate from 25 to 26 kaBP ( $PR_{14\text{C}} = 2.1 \cdot 10^4 \text{ atoms} \cdot \text{cm}^{-2}\text{s}^{-1}$ ). For this and in most of the transient simulations, we use the most recent production rate time series developed by Hain et al. (2014). In a sensitivity analysis, the  $^{14}\text{C}$  production rates from the studies by Laj et al. (2004) and Muscheler et al. (2004) are applied as well. A description of the main characteristics of these data is given in the Supplement.

~~The equatorward expansion of terrestrial ice sheets is set to~~ LGM climate reconstructions show that the Laurentide ice sheet expanded as far south as 38° N (see e.g. Peltier, 2004). To account for this and the lack of an ice sheet in large parts of Siberia, and within the constraints of our zonally-averaged one hemisphere model, we prescribe the southernmost ice sheet extent to be 47° latitude for generating LGM conditions. This is within the uncertainty range of LGM climate reconstructions (see e.g. Peltier, 2004) and has to be understood as a global two hemisphere average. For the transient simulations, we impose the temporal retreat of the ice line to the disappearance of the ice sheets at 70° latitude during the Holocene. For this, we linearly prescribe  $L_{ice}$  (see Sects. 2.3 and 2.4) to a data set presented in Shakun et al. (2012) showing the Northern Hemisphere (NH) ice sheet expansion from 100% (ice line at 47°) at the LGM to 0% (ice line at 70°) at present day. An example case for  $L_{ice}$  and  $L_{snow}$  in a transient simulation is given in the Supplement.

A model analogy to isolated deep water in the SO (see e.g. Watson and Naveira Garabato, 2006) is generated through application of a depth-dependent function for vertical exchange intensity in the high latitude ocean sector. For this, we impose a sharp decrease in vertical diffusion at around 1800m ocean depth which limits mixing of the upper ocean layers with intermediate and deep ocean waters. The transition depth of this profile was varied to obtain LGM climate conditions that constrain all required oceanic and atmospheric variables. Through the application of this diffusivity profile, the isolated ocean waters below the transition change towards high dissolved inorganic carbon and alkalinity values as well as towards low oxygen concentrations and  $^{13,14}\text{C}$  isotope ratios. This variation in vertical exchange intensity should not be understood as a change in real oceanic vertical diffusion, but rather as a model analogy for LGM conditions of the SO that were likely due to some combination of weakened or equatorward shifted westerly winds (Toggweiler and Russel, 2008; Anderson et al., 2009; d'Orgeville et al., 2010) and increased stratification through brine-induced effects (Bouttes et al., 2010, 2011; Mariotti et al., 2013). With its wide latitudinal extent and the land bounding poleward of 70°, the high latitude ocean sector of the DCESS model bears considerable resemblance to the SO. During the transient simulations, we slowly restore this modification back toward PI conditions between 17.5 and 14.5 kaBP to apply the entire effect of this process to the MI. In this process, deeper layers in the high latitude ocean sector are again brought in contact with surface layers promoting outgassing and ocean profiles

go back toward the initial PI state shown in Shaffer et al. (2008). An illustration of the profile as well as a detailed technical description of the procedure and some additional information are presented in the [supplementary material Supplement](#).

When all these adaptations, plus a few minor changes (described in the Supplement), are applied, an 80 ka DCESS simulation leads to a steady climate state with conditions close to data-based LGM reconstructions. Atmospheric  $p\text{CO}_2$  decreases to 187.9 ppm and the global mean atmosphere temperature to 11.70 °C. For  $p\text{CO}_2$ , proxy data records by Lüthi et al. (2008) provide a range of 186 – 198 ppm and Shakun et al. (2012) present LGM global mean atmosphere temperatures between 11.5 and 11.8 °C. Moreover, atmospheric isotope ratios of  $\delta^{13}\text{C} = -6.41\text{‰}$  and  $\Delta^{14}\text{C} = 414.5\text{‰}$  and low oxygen values but no widespread anoxia in the deep ocean are achieved. This agrees well with proxy data records presented by Schmitt et al. (2012) [and Reimer et al. \(2013\)](#), [Reimer et al. \(2013\)](#) and [Jaccard et al. \(2014\)](#). An overview of these data and the ocean profiles for LGM conditions of various variables for the high and the low-mid latitude sector [are shown is given](#) in the Supplement. In the following sections, we present analyses of the transient simulations from the LGM to the Holocene, using the transition functions described above.

### 3.2 Transient simulation results

~~Four transient simulations have been conducted to assess the impacts~~ [To evaluate the impact](#) of the individual [transition functions on atmospheric  \$T\_{glob}\$ ,  \$p\text{CO}\_2\$ ,  \$\delta^{13}\text{C}\$  and  \$\Delta^{14}\text{C}\$  changes](#). The transition functions described above were applied sequentially to better assess the impact of each process. These simulations show that during the of the MI, all the above described processes together generate a change of  $p\text{CO}_2$  [new model developments, we carried out six transient simulations starting from LGM conditions as described above, varying the following parts of the model land biosphere: The first simulation features a nul-vegetation model \(Nul\\_veg\), meaning that the vegetation does not change from LGM conditions and land-atmosphere carbon \(including the rare isotopes\) fluxes are suppressed. Then, we use the old uniform land biosphere scheme \(Old\\_bio\) \(including the snow/ice line-based reduction of biosphere area, see Sect. 2.5, but no permafrost parameterisation\), global temperature,  \$-0.18\text{‰}\$   \$\delta^{13}\text{C}\$  and  \$-85\text{‰}\$   \$\Delta^{14}\text{C}\$  \(see Supplement\). This is only about half of the change that data-based reconstructions show. Most of the simulated changes can be attributed to the resumption of the ocean high latitude vertical diffusion and the thereby induced outgassing of the carbon-rich and isotopically depleted deep waters. Our DCESS simulations reproduce some aspects of the early last deglaciation, while others are still underestimated because important processes are either missing or not adequately represented.](#)

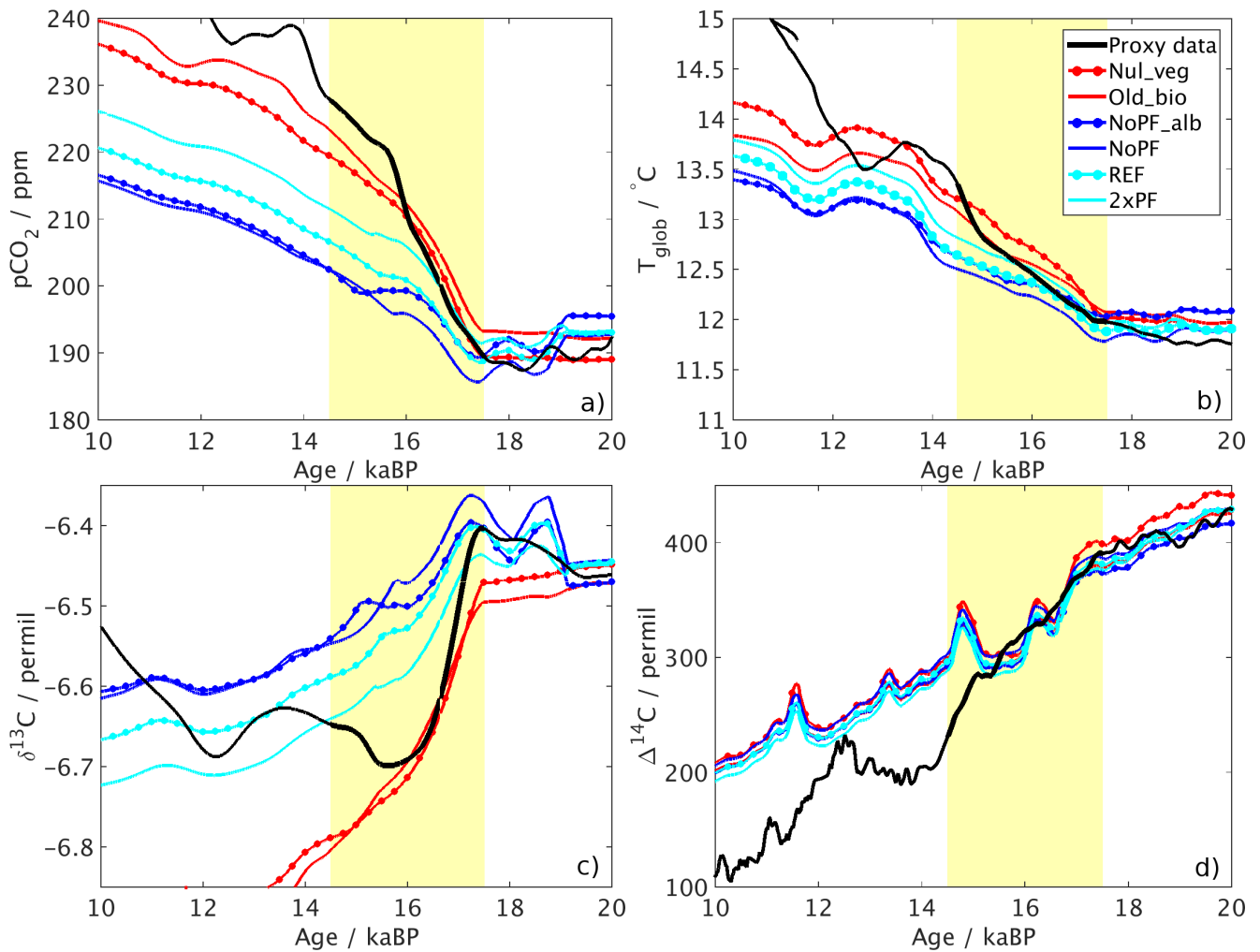
In order to evaluate how much influence permafrost has on the atmospheric quantities, we now deactivate the permafrost in the computation of the atmosphere-terrestrial biosphere fluxes (No\_PF, no influence of permafrost). For this, we set the [additional and subsequently the new scheme without the permafrost](#) (permafrost-atmosphere carbon (including the rare isotopes) fluxes to zero throughout the simulation with all changes (the All\_TF simulation, see Supplement). Fig. 5 shows the results of these simulations and moreover, those of a simulation with the same conditions, but with the old uniform fluxes set to zero) and the new albedo features (NoPF\_alb) and then the same but including the new albedo (NoPF). Last, we performed simulations with all the new model developments (REF) plus a further sensitivity experiment with a doubled ( $60\text{ GtC} \cdot \text{m}^{-2}$ ) permafrost carbon reservoir, as already mentioned above. An overview of these simulations is provided in table 3.

<u>Simulation</u>	<u>Long name</u>	<u>Setup</u>
<u>Nul_veg</u>	<u>Nul vegetation</u>	<u>Suppressed land-atmosphere fluxes</u>
<u>Old_bio</u>	<u>Old biosphere</u>	<u>Original uniform DCESS land biosphere scheme (<del>Old_bio</del>) which does also not feature the parameterisation for</u> <u>(No permafrost and no land area change)</u>
<u>NoPF_alb</u>	<u>No permafrost</u> <u>No albedo</u>	<u>Supressed fluxes from permafrost and</u> <u>old (not vegetation-dependent) albedo</u>
<u>NoPF</u>	<u>No permafrost</u>	<u>Supressed fluxes from permafrost</u>
<u>REF</u>	<u>Reference</u>	<u>Including all new developments as described in the text</u>
<u>2xPF</u>	<u>Doubled permafrost</u>	<u>As REF but with two times the estimate for permafrost carbon reservoir</u>

**Table 3.** Overview of the DCESS model simulations with short description.

The results of these model simulations as well as data-based reconstructions are presented in Fig. 5 from 20 to 10 kaBP.  
As our transition functions (in particular the upwelling of the deep ocean) are tailor-made for simulating the Mystery Interval  
between 17.5 and 14.5 kaBP, we particularly focus in our analysis on this 3 ka slice of the last glacial termination.

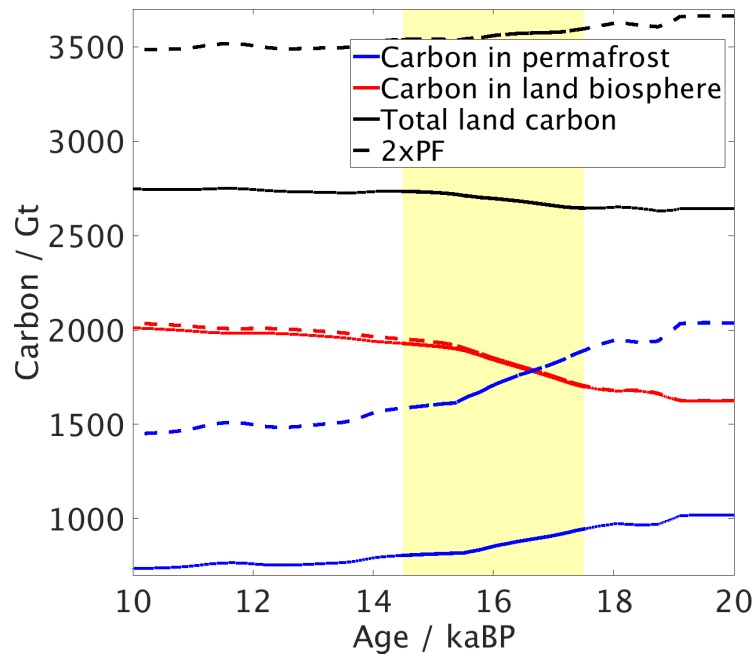
In the simulation without the influence of permafrost, a reduction of the change  
5 The nul vegetation model shows the larges  
atmospheric changes across the MI. Uptake of carbon through the land biosphere does not take place in this simulation,  
therefore, all outgassed carbon stays in the atmosphere and amplifies global warming. This also reflects in the  $\delta^{13}\text{C}$  and  $\Delta^{14}\text{C}$   
curves, isotopically strongly depleted carbon from the deep ocean decreases the atmospheric isotope ratios. Especially the far  
too strong drop in  $\delta^{13}\text{C}$  in the nul vegetation simulation points out that the regrowth of the biosphere and its preferential uptake  
of  $^{12}\text{C}$  keeps  $\delta^{13}\text{C}$  at a reasonable level in the other simulations, although the increase after 12 kaBP is not represented well  
10 in the model. The simulation with the old land biosphere scheme shows comparable changes  
across the MI~~can be observed~~  
~~in all four atmospheric variables compared to the reference simulation~~All\_TF, the missing expansion of the biosphere leads  
to a strong increase of atmospheric  $p\text{CO}_2$ . The change is even somewhat larger than in the Nul\_veg simulation, because the  
land biomass decreases due to the warming (see also Sect. 2.5). Due to its reaction on vegetation changes, the new albedo  
diversification leads to stronger warming. This also generates some stronger  $p\text{CO}_2$  increase. When we enable the permafrost  
15 parameterisation in the REF simulation,  $p\text{CO}_2$  rises around 2.6 ppm more and the global mean atmosphere temperature around  
0.1 ° C. The results of the two simulations start diverging at around 19 kaBP. This is when the change in ice sheet extent leads  
to first clear variations through its effect on the permafrost parameterisation in the model (see Fig. S4-S3 in the Supple-  
ment). Across the MI, the~~The~~isotope ratios are only slightly affected by these new features, in particular  $\Delta^{14}\text{C}$  is controled  
mostly by the changes of the stratospheric production rate of  $^{14}\text{C}$ . The sensitivity experiment with a doubled permafrost  
20 reservoir shows a further increase of  $p\text{CO}_2$ . The difference between the two lines additionally increases in all four panels  
and only slightly thereafter. Until the year , the permafrost component accounts for an additional change of around in  
2xPF  
and the REF simulations is larger than between the REF and the noPF simulation. The biosphere regrowth and its carbon



**Figure 5.** Atmospheric values for the DCESS ~~simulation-simulations~~ with ~~all transition functions~~ nul vegetation model (AllNul\_FFveg., red line with dots), see Supplement ~~old biosphere scheme (Old\_bio, red line), deactivated permafrost component and old albedo scheme (NoPF\_alb, blue line with dots), deactivated permafrost component and new albedo scheme (NoPF, blue line), reference simulation with all new components (REF, light blue line with dots) and sensitivity experiment with doubled permafrost carbon reservoir (2xPF, light blue line), and data-based reconstructions (black);~~ pCO<sub>2</sub> by Lüthi et al. (2008), temperatures by Shakun et al. (2012), δ<sup>13</sup>C by Schmitt et al. (2012) and Δ<sup>14</sup>C by Reimer et al. (2013). ~~Blue line: DCESS simulation with all transitions functions, but deactivated permafrost component (No\_PF).~~ ~~Cyan line: Same simulation with the old terrestrial biosphere scheme (Old\_bio).~~

uptake is only slightly enhanced in the 2xPF simulation. However, some more change already happens before, i.e. after 19 kaBP. Therefore, this shows that uncertainties of that kind can have a considerable impact on climate change simulations. In comparison to data-based reconstructions, the MI atmospheric changes are closest in the 2xPF simulation (disregarding

the Nul\_veg simulation). More than half of the  $p\text{CO}_2$  (6.8% of the change during the MI), about in global mean atmosphere temperature, and only  $-0.01\text{‰}$  and the global mean temperature changes are represented and the drop in  $\delta^{13}\text{C}$  and  $-2\text{‰}$  in  $\Delta^{14}\text{C}$ . This indicates, that for the overall climate change across the MI, permafrost plays only a secondary role, with relatively small contributions to temperature and isotopes.  $\Delta^{14}\text{C}$  is not sensitive to changes in vegetation and hence the influence of its release from permafrost dominates its development.  $\Delta^{14}\text{C}$  shows only little sensitivity to our new model developments.



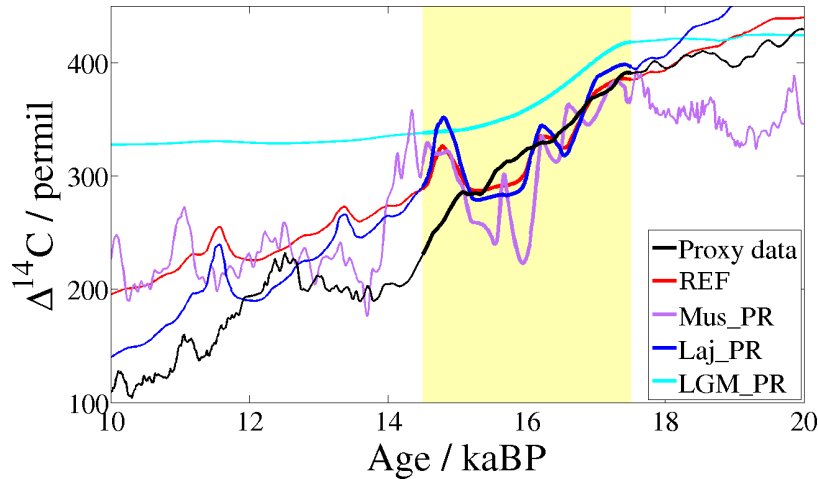
**Figure 6.** Carbon stored in soil below permafrost and in the terrestrial biosphere as well as their sum for the All\_TF-REF and for the 2xPF simulation.

Fig. 6 shows the changes of permafrost carbon, land biosphere carbon and their sum for the All\_TF-simulation. In this REF and the 2xPF simulations. In the REF simulation, carbon uptake through the regrowth of the biosphere across the MI slightly exceeds (by 70 GtC) carbon outgassing through ice sheet retreat and permafrost thawing then. In the 2xPF simulation, the permafrost carbon change slightly outweighs the vegetation effect. This demonstrates that the two mechanisms actually broadly compensate each other. Each of these changes, however, is subject to considerable uncertainty. As mentioned above, the land biosphere carbon reservoir change in the model is at the low end of the range found in other studies (Peng et al., 1998; Prentice et al., 2014) and provides an estimate of the uncertainty of the role of permafrost in our results. Also, model carbon release of 337 GtC from permafrost is lower than that of Ciais et al. (2012), who found a 700 GtC difference between LGM and present day global permafrost carbon reservoir. Our lower estimate may seem to be related to our simplified permafrost treatment that used estimates of the extent of land area covered by ice sheets as well as and the simple assumption of 30 kg of available carbon per square meter of permafrost covered area (Schuur et al., 2008). The sensitivity

simulation with  $60 \text{ kgC} \cdot \text{m}^{-2}$  in permafrost provides more realistic values for permafrost carbon release (667 GtC) and also for the global carbon reservoir ( $\sim 3600 \text{ GtC}$ , see also Sect. 2.5).

In addition, we conducted four transient simulations to assess the impacts of the individual transition functions on atmospheric  $T_{\text{glob}}$ ,  $p \text{CO}_2$ ,  $\delta^{13} \text{C}$  and  $\Delta^{14} \text{C}$  changes (see Supplement). The transition functions described above were applied sequentially to better assess the impact of each process. These simulations show that during the 3 ka of the MI most of the simulated changes can be attributed to the resumption of the ocean high latitude vertical diffusion and the thereby induced outgassing of the carbon-rich and isotopically depleted deep waters. Our DCESS simulations reproduce only some aspects of the early last deglaciation, while others are underestimated because important processes are either missing or not adequately represented.

As has been mentioned above, the change in  $\Delta^{14} \text{C}$  during the MI in the All\_TF\_REF simulation is not as large as in the data-based reconstructions and not sensitive to our new developments of the land biosphere. Apart from atmospheric  $\text{CO}_2$  itself and the release of deep ocean waters,  $\Delta^{14} \text{C}$  is strongly influenced by the cosmogenic production rate of  $^{14} \text{C}$ . This production rate is determined with rather large uncertainties and there are different ways to derive it. In the Supplement, we present the three  $^{14} \text{C}$  production rate time series of the studies by Laj et al. (2004); Muscheler et al. (2004) and Hain et al. (2014) across the last 25 kaBP. Here, we present an evaluation of the three  $^{14} \text{C}$  production rate data applied to the reference simulation. In Fig. 7, we show the simulations with the three different production rates, as well as for a simulation with constant LGM-value production rate (Mus\_PR, Muscheler et al. (2004) production rate; Laj\_PR, Laj et al. (2004) production rate; LGM\_PR, constant LGM-value production rate). The proxy data record by Reimer et al. (2013) is also included in the figure.



**Figure 7.**  $\Delta^{14} \text{C}$  in transient simulations with all changes (see Sect. 3.1) applying different  $^{14} \text{C}$  production rates from Hain et al. (2014) (red, REF), Muscheler et al. (2004) (magenta, Mus\_PR), Laj et al. (2004) (blue, Laj\_PR), Hain et al. (2014) (red, All\_TF) and fixed LGM production rate (cyan, LGM\_PR), and data based reconstructions from Reimer et al. (2013) (black).

The simulation with constant  $^{14}\text{C}$  production rate at LGM level shows a  $\Delta^{14}\text{C}$  drop by 80‰ from the beginning to the end of the MI, almost entirely through the outgassing of isotopically depleted deep ocean waters. ~~Neither~~ None of the  $^{14}\text{C}$  production rates can account for the remaining 80‰ reduction to explain the  $\Delta^{14}\text{C}$  decrease of 160‰ across the MI that can be seen in the data-based reconstruction by Reimer et al. (2013). With the data set by Hain et al. (2014),  $\Delta^{14}\text{C}$  drops by 96‰, using the Laj et al. (2004) data, a 105‰ decrease can be explained and the Muscheler et al. (2004) time series only leads to -58‰ change. Furthermore, the proxy data does not show the production rate-caused variations within the MI and also, in the Mus\_PR simulation, atmospheric  $\Delta^{14}\text{C}$  shows a large and sudden drop of around 150‰ shortly after the MI between 14.3 and 13.7 kaBP.

### 3.3 Discussion of transient simulations

The model reproduces ~~around more than~~ half of the MI changes in atmospheric  $p\text{CO}_2$ ,  $T_{glob}$ ,  $\delta^{13}\text{C}$  and  $\Delta^{14}\text{C}$  as shown in data-based reconstructions. ~~Most of these changes are caused by the upward transport of carbon-rich and isotopically depleted waters from the deep ocean through prescription of the vertical diffusion profile and its resumption, but also other processes play important roles. The dust component accounts for about global temperature change during the MI. Since the other atmospheric quantities are only moderately affected by dust, most of that is can be related to the direct dust radiative forcing. The  $\delta^{13}\text{C}$  drop at the onset of~~ Overall, the representation of the land biosphere is shown to play an important role in the interplay of many processes. The model results reach from 12 to 31 ppm change in  $p\text{CO}_2$  across the MI, i.e. from less than a third of the change presented in data-based reconstructions to more than 80%. The "best" results are reached for simulation using no biosphere fluxes or the original DCESS model biosphere module. However, these "best" results are obtained unambiguously for the wrong reasons. The missing uptake of carbon through the land biosphere for these simulations and the deglaciation is fairly well represented by this DCESS modelling approach and also mainly caused by deep ocean mixing. Also Brovkin et al. (2002) point out the importance of oceanic processes for atmospheric unrealistic behaviour of the old biosphere scheme to temperature changes lead to too high  $p\text{CO}_2$  and temperature values. The  $\delta^{13}\text{C}$  at glacial-interglacial time scales. However, after around, isotope ratios reveal this model deficiency.  $\delta^{13}\text{C}$  increases again in the observations, while it remains relatively constant in the simulations further decreases in the Nul\_veg and old biosphere simulations after the MI, while in all other simulations,  $\delta^{13}\text{C}$  stagnates. In the data-based reconstructions,  $\delta^{13}\text{C}$  even rises again. Schmitt et al. (2012) mainly attribute this rise to the continuing regrowth of the land biosphere, which does not have such a strong effect on atmospheric  $\delta^{13}\text{C}$  in the model. According to Crichton et al. (2016), also peatlands could account for this effect, those however, are not included in our vegetation scheme. When we apply the double of the estimate of  $30\text{ GtC} \cdot \text{m}^{-2}$  from Ciais et al. (2012) the model results considerably improve in comparison with data-based reconstructions. In consideration of the apparent underestimation of total land biosphere carbon as shown in Sect. 2.5 and the large uncertainties in the estimation by Ciais et al. (2012), the usage of  $60\text{ GtC} \cdot \text{m}^{-2}$  is still reasonable.

The impact of ~~permafrost the land biosphere~~ on  $\Delta^{14}\text{C}$  is very small, even though we assume carbon released from permafrost to be radiocarbon free. The expected radiocarbon decrease generated through permafrost thawing can apparently be compensated by ocean-atmosphere exchange and subsequent mixing to the deeper ocean. It has to be considered that the car-

bon buried below permafrost seems to be underestimated in our model approach compared to a study by Ciais et al. (2012) and that interhemispheric see-saw effects can affect the timing of extensive permafrost ( $^{14}\text{C}$  depleted) carbon release, especially during HE1 (see e.g. Köhler et al., 2014). The much discussed sharp  $\Delta^{14}\text{C}$  drop of 160‰ (see Reimer et al., 2013) (note that in previous studies by Broecker and Barker (2007) or Reimer et al. (2009) this was referred to as 190‰) at the early stages of the last deglaciation is not entirely reproduced by this modelling study. By applying a constant LGM  $^{14}\text{C}$  production rate, all the above described processes can account for about 70‰ change. None of the three different time series of the  $^{14}\text{C}$  production rate can account for the rest of the  $\Delta^{14}\text{C}$  change. At most, the data by Laj et al. (2004) leads to an additional 25‰ decrease. However, the determination of the  $^{14}\text{C}$  production rate is obviously subject to large uncertainties. For example, the drop in the Muscheler et al. (2004) time series at around 14 kaBP leads to a sudden 150‰ decrease in  $\Delta^{14}\text{C}$  in our model simulation but can not be seen in  $\Delta^{14}\text{C}$  proxy data. In this context, it should be mentioned, that recent revisions to ice core time scales have not yet been applied for revising the reconstructed snow accumulation rates and  $^{10}\text{Be}$  fluxes and its influence on the  $^{10}\text{Be}$ -based  $^{14}\text{C}$  production rate (R. Muscheler, personal communication, 2015).

Most of the MI changes are caused by the upward transport of carbon-rich and isotopically depleted waters from the deep ocean through prescription of the vertical diffusion profile and its resumption. The dust component accounts for about 0.3 °C global temperature change during the MI. Since the other atmospheric quantities are only moderately affected by dust, most of that can be related to the direct dust radiative forcing. To account for the other half of changes that our simulations can not reproduce, several processes can be thought of being insufficiently represented in the model and moreover, this could also be due to the timing of one or more of the transition functions, underrepresenting effects during the MI. Brovkin et al. (2007); Kohfeld and Ridgwell (2009) and Mariotti et al. (2013) discuss a number of processes that combined can account for the entire deglaciation, although with sometimes large uncertainties, not all of them were captured in our study. E.g., enhanced ocean remineralisation length scales during the glacial, due to less active bacteria at low temperatures, could trap more dissolved inorganic carbon in the deep ocean, which then could account for additional  $\text{CO}_2$  outgassing but would also reduce deep ocean dissolved oxygen concentrations. Also the volume of isolated deep waters in the SO is uncertain and moreover, water masses in other oceans may also have contributed to the overall atmospheric  $p\text{CO}_2$  change (Rose et al., 2010; Okazaki et al., 2010; Kwon et al., 2012; Huiskamp and Meissner, 2012). The  $T_{\text{glob}}$  and  $p\text{CO}_2$  changes after the MI across the BA, the Younger Dryas and the Holocene are not expected to be simulated in detail by the DCESS model. Due to the model's simplified geometry, interactions between the hemispheres and thus the bipolar seesaw can not be represented. The simplicity of DCESS model ocean dynamics also limit feedbacks of ocean-atmosphere interactions that may have contributed to the overall carbon cycle change during the MI. For instance, Mariotti et al. (2016) discuss the effect of North Atlantic freshening through ice sheet melting inducing upper water stratification and subsequent prevention of carbon uptake by the ocean ~~to~~ that could contribute to enhanced  $p\text{CO}_2$  ~~during HE1~~ at the end of the MI. An alternative approach would be to use 3-D modelling to deal specifically with one or more of the processes listed above. However, this would involve other types of uncertainties like the strength and position of the Southern Westerly Winds and the parameterisation of diapycnal mixing.

#### 4 Summary and conclusions

The land biosphere scheme that accounts for  $^{12,13,14}\text{C}$  cycling with leaf, wood, litter and soil of the reduced complexity Earth System Model DCESS has been extended to three different vegetation zones. Based on a complex land biosphere model study, we defined dynamically varying vegetation borders on a global scale that depend on temperature variations. We also introduce a parameterisation that accounts for carbon, including its rare isotopes, that is being trapped below the permafrost as well as below terrestrial ice sheets for glacial conditions and released during deglaciation events. In an evaluation, the new terrestrial biosphere scheme is shown to simulate more realistic global biomass size and timing in climate change experiments, and thereby significantly improves the representation of land-atmosphere carbon exchange rates in the DCESS model. For climate change studies on glacial-interglacial time scales, these aspects can be crucial when analysing the contributions and interactions of processes controlling carbon exchange between land, atmosphere and ocean.

For a first application of the new biosphere parameterisation, the model is first tuned to Last Glacial Maximum conditions to subsequently carry out transient simulations across the last glacial termination. Along with a number of established adaptations of physical and biogeochemical parameters, the DCESS model successfully reproduces proxy data records of glacial conditions in the ocean and atmosphere when we impose the isolation of high latitude deep ocean waters. For the transient model simulations, we have additionally developed a set of explicit functions that describe the transitions of atmospheric dust, ocean volume and terrestrial ice sheet extent across the last 25 kaBP. These sensitivity experiments show that large parts of the exceptional change in atmospheric  $p\text{CO}_2$ ,  $\delta^{13}\text{C}$ ,  $\Delta^{14}\text{C}$  and  $T_{glob}$  at the onset of the last glacial termination (Mystery Interval, 17.5-14.5 kaBP) can be represented by this approach. Some variations as seen in data-based reconstructions can not be reproduced by our model study. These remaining changes could possibly be captured by applying a dynamically more complex model including distinct water masses and a second hemisphere for representing bipolar seesaw effects, or by revising and/or adding one or more model parameterisations. New insights into these mechanisms can help to improve our understanding of global carbon cycle changes on centennial to millennial time scales.

The thawing of permafrost due to atmospheric warming and retreat of ice sheets, as well as the regrowth of the terrestrial biosphere, are found to play moderate, but important roles in explaining the climate change of this period of the last deglaciation. We found that these two processes broadly compensate each other in the model in terms of  $\text{CO}_2$  exchange with the atmosphere, making little net contribution to atmospheric  $p\text{CO}_2$  changes across the last transition. However, since our simulation bears considerable uncertainties, we also found that particularly the permafrost component could be underestimated. Simulations across the transition using the original DCESS land biosphere model also showed essentially no net contribution to atmospheric  $p\text{CO}_2$  change as reflected in the very small change in land biomass between LGM and present day. But with the new biosphere module (including permafrost) this result is obtained in a more correct manner, in better agreement with proxy data and more complex modelling results.

Supplementary material related to this article is available online at doi:10.5194/gmd-0-1-2017-supplement.

*Code and data availability:* The DCESS model code is available at <http://www.dcess.dk/> and all applied data are available as referenced.

*Acknowledgements.* We thank Raimund Muscheler for providing  $^{14}\text{C}$  production rate data and information about it as well as Ricardo De Pol-Holz for discussions. This work was financed by Chilean Nucleus NC120066. GS and NA acknowledge support by FONDECYT grants # 1120040 and # 1150913, MR by Fondecyt grant # 1131055, and FL by Fondecyt grant # 1151427.

## References

- Adams, J. M., Faure, H., Faure-Denard, L., McGlade, J. M., and Woodward, F. I.: Increase in terrestrial carbon storage from the Last Glacial Maximum to the present, *Nature*, 348, 711–714, doi:10.1038/348711a0, 1990.
- Adkins, J. F. and Schrag, D. P.: Reconstructing Last Glacial Maximum bottom water salinities from deep-sea sediment pore fluid profiles, *Earth and Planetary Science Letters*, 16, 109–123, doi:10.1016/S0012-821X(03)00502-8, 2002.
- Adkins, J. F., McIntyre, K., and Schrag, D. P.: The Salinity, Temperature, and  $\delta^{18}\text{O}$  of the Glacial Deep Ocean, *Science*, 298, 1769–1773, doi:10.1038/35038000, 2002.
- Anderson, R. F., Ali, S., Bradtmiller, L., Nielsen, S. H. H., Fleisher, M. Q., Anderson, B. E., and Buckle, L. H.: Wind-Driven Upwelling in the Southern Ocean and the Deglacial Rise in Atmospheric  $\text{CO}_2$ , *Science*, 323, 1443–1448, doi:10.1126/science.1167441, 2009.
- Annan, J. D. and Hargreaves, J. C.: A new global reconstruction of temperature changes at the Last Glacial Maximum, *Climate of the Past*, 9, 367–376, doi:10.5194/cp-9-367-2013, 2013.
- Bonan, G. B.: Forests and Climate Change: Forcings, Feedbacks, and the Climate Benefits of Forests, *Science*, 320, 1444, doi:10.1126/science.1155121, 2008.
- Bouttes, N., Paillard, D., and Roche, D. M.: Impact of brine-induced stratification on the glacial carbon cycle, *Climate of the Past*, 6, 681–710, 2010.
- Bouttes, N., Paillard, D., Roche, D. M., Brovkin, V., and Bopp, L.: Last Glacial Maximum  $\text{CO}_2$  and  $\delta^{13}\text{C}$  successfully reconciled, *Geophysical Research Letters*, 38, L02705, doi:10.1029/2010GL044499, 2011.
- Broecker, W. and Barker, S.: A 190‰ drop in atmosphere's  $\Delta^{14}\text{C}$  during the "Mystery Interval" (17.5 to 14.5 kyr), *Earth and Planetary Science Letters*, 256, 90–99, doi:10.1016/j.epsl.2007.01.015, 2007.
- Brovkin, V., Hofmann, M., Bengtson, J., and Ganopolski, A.: Ocean biology could control atmospheric  $\delta^{13}\text{C}$  during glacial-interglacial cycle, *Geochemistry Geophysics Geosystems*, 3(5), doi:10.1029/2001GC000270, 2002.
- Brovkin, V., Ganopolski, A., Archer, D., and Rahmstorf, S.: Lowering of glacial atmospheric  $\text{CO}_2$  in response to changes in oceanic circulation and marine biogeochemistry, *Paleoceanography*, 22, PA4202, doi:10.1029/2006PA001380, 2007.
- Burke, A. and Robinson, L. F.: The Southern Ocean's Role in Carbon Exchange During the Last Deglaciation, *Science*, 335, 557–561, doi:10.1126/science.1208163, 2012.
- Chapin, I. I. I., Stuart, F., Matson, P. A., and Vitousek, P.: Principles of terrestrial ecosystem ecology, 2011.
- Ciais, P., Tagliabue, A., Cuntz, A., Bopp, L., Scholze, M., Hoffmann, G., Lourantou, A., Harrison, S. P., Prentice, I. C., Kelley, D. I., Koven, C., and Piao, S. L.: Large inert carbon pool in the terrestrial biosphere during the Last Glacial Maximum, *Nature Geoscience*, 5, 74–79, doi:10.1038/ngeo1324, 2012.
- Crichton, K. A., Roche, D. M., Krinner, G., and Chappellaz, J.: A simplified permafrost-carbon model for long-term climate studies with the CLIMBER-2 coupled earth system model, *Geoscientific Model Development*, 7, 3111–3134, doi:10.5194/gmd-7-3111-2014, 2014.
- Crichton, K. A., Bouttes, N., Roche, D. M., Chappellaz, J., and Krinner, G.: Permafrost carbon as a missing link to explain  $\text{CO}_2$  changes during the last deglaciation, *Nature*, 9, 683–687, doi:10.1038/NGEO2793, 2016.
- Curry, W. B. and Oppo, D. W.: Glacial water mass geometry and the distribution of  $\delta^{13}\text{C}$  of  $\sum\text{CO}_2$  in the western Atlantic Ocean, *Paleoceanography*, 20, PA1017, doi:10.1029/2004PA001021, 2005.
- Davidson, E. A. and Janssens, I. A.: Temperature sensitivity of soil carbon decomposition and feedbacks to climate change, *Nature*, 440(7081), 165–173, doi:10.1038/nature04514, 2006.

- d'Orgeville, M., Sijp, W. P., England, M. H., and Meissner, K. J.: On the control of glacial-interglacial atmospheric CO<sub>2</sub> variations by the Southern Hemisphere westerlies, *Geophysical Research Letters*, 37, L21 703, doi:10.1029/2010GL045261, 2010.
- Eby, M., Weaver, A. J., Alexander, K., Zickfeld, K., Abe-Ouchi, A., Cimadoribus, A. A., Crespin, E., Drijfhout, S. S., Edwards, N. R., Eliseev, A. V., Feulner, G., Fichet, T., Forest, C. E., Goosse, H., Holden, P. B., Joos, F., Kawamiya, M., Kicklighter, D., Kienert, H., Matsumoto, K., Mokhov, I. I., Monier, E., Olsen, S. M., Pedersen, J. O. P., Perrette, M., Philippon-Berthier, G., Ridgwell, A., Schlosser, A., Schneider, T., von Deimling, G., Shaffer, G., Smith, R. S., Spahni, R., Sokolov, A. P., Steinacher, M., Tachiiri, K., Tokos, K., Yoshimori, M., Zeng, N., and Zhao, F.: Historical and idealized climate model experiments: an intercomparison of Earth system models of intermediate complexity, *Climate of the Past*, 9, 1111–1140, doi:10.5194/cp-9-1111-2013, 2013.
- Fischer, H., Schmitt, J., Lüthi, D., Stocker, T. F., Tschumi, T., Parekh, P., Joos, F., Köhler, P., Völker, C., Gersonde, R., Barbante, C., Le Floch, M., Raynaud, D., and Wolff, E.: The role of Southern Ocean processes on orbital and millennial CO<sub>2</sub> variations - a synthesis, *Quaternary Science Reviews*, 29 (1), 193–205, doi:10.1016/j.quascirev.2009.06.007, 2010.
- Francois, R., Altabet, M. A., Yu, E.-F., Sigman, D. M., Bacon, M. P., Frank, M., Bohrmann, G., Bareille, G., and Labeyrie, L. D.: Contribution of Southern Ocean surface-water stratification to low atmospheric CO<sub>2</sub> concentrations during the last glacial period, *Nature*, 389, 929–935, doi:10.1038/40073, 1997.
- Friedlingstein, P., Cox, P., Betts, R., Bopp, L., von Bloh, W., Brovkin, V., Cadule, P., Doney, S., Eby, M., Fung, I., Bala, G., John, J., Jones, C., Joos, F., Kato, T., Kawamiya, M., Knorr, W., Lindsay, K., Matthews, H. D., Raddatz, T., Rayner, P., Reick, C., Roeckner, E., Schnitzler, K.-G., Schnur, R., Strassmann, K., Weaver, A. J., Yoshikawa, C., and Zeng, N.: Climate-carbon cycle feedback analysis: Results from the C<sup>4</sup>MIP model Intercomparison, *Journal of Climate*, 19, 3337–3353, doi:10.1175/JCLI3800.1, 2006.
- Gerber, S., Joos, F., and Prentice, C.: Sensitivity of a dynamic global vegetation model to climate and atmospheric CO<sub>2</sub>, *Global Change Biology*, 10, 1223–1239, doi:10.1111/j.1365-2486.2004.00807.x, 2004.
- Gower, S. T., Kucharik, C. J., and Norman, J. M.: Direct and indirect estimation of leaf area index,  $f_A PAR$ , and net primary production of terrestrial ecosystems, *Remote sensing of environment*, 70, 29–51, doi:10.1016/S0034-4257(99)00056-5, 1999.
- Hain, M. P., Sigman, D. M., and Haug, G. H.: Distinct roles of the Southern Ocean and North Atlantic in the deglacial atmospheric radiocarbon decline, *Earth and Planetary Science Letters*, 394, 198–208, doi:10.1016/j.epsl.2014.03.020, 2014.
- Hartmann, D. L.: *Global Physical Climatology*, Elsevier, New York, 357pp, 1994.
- Huiskamp, W. N. and Meissner, K. J.: Oceanic carbon and water masses during the Mystery Interval: A model-data comparison study, *Paleoceanography*, 27, PA4206, doi:10.1029/2012PA002368, 2012.
- Jaccard, S. L., Galbraith, E. D., Fröhlicher, T. L., and Gruber, N.: Ocean (de)oxygenation across the last deglaciation: Insights for the future, *Oceanography*, 27 (1), 26–35, doi:10.5670/oceanog.2014.05, 2014.
- Joos, F., Gerber, S., Prentice, I. C., Otto-Bliesner, B. L., and Valdes, P. J.: Transient simulations of Holocene atmospheric carbon dioxide and terrestrial carbon since the Last Glacial Maximum, *Global Biogeochemical Cycles*, 18, GB2002, doi:10.1029/2003GB002156, 2004.
- Khvorostyanov, D. V., Ciais, P., Krinner, G., and Zimov, S. A.: Vulnerability of east Siberia's frozen carbon stores to future warming, *Geophysical Research Letters*, 35, L10 703, doi:10.1029/2008GL033639, 2008.
- Kohfeld, K. E. and Ridgwell, A.: Glacial-Interglacial Variability in Atmospheric CO<sub>2</sub>, *Geophysical Research Series*, 187, 251–286, doi:10.1029/2008GM000845, 2009.
- Köhler, P., Bintanja, R., Fischer, H., Joos, F., Knutti, R., Lohmann, G., and Masson-Delmotte, V.: What caused Earth's temperature variations during the last 800,000 years? Data-based evidence on radiative forcing and constraints on climate sensitivity Permafrost thawing as a possible source of abrupt, *Quat. Sci. Rev.*, 29, 129–145, doi:10.1016/j.quascirev.2009.09.026, 2010.

- Köhler, P., Knorr, G., and Bard, E.: Permafrost thawing as a possible source of abrupt carbon release at the onset of the Bølling/Allerød, *Nature Communications*, 5, 5520, doi:10.1038/ncomms6520, 2014.
- Kwon, E. Y., Hain, M. P., Sigman, D. M., Galbraith, E. D., Sarmiento, J. L., and Toggweiler, J. R.: North Atlantic ventilation of "southern-sourced" deep water in the glacial ocean, *Paleoceanography*, 27, PA2208, doi:10.1029/2011PA002211, 2012.
- 5 Laj, C., Kissel, C., and Beer, J.: High resolution global paleointensity stack since 75 kyr (GLOPIS-75) calibrated to absolute values, in: *Geophysical Monograph Series (AGU)*, 145, 255–265, doi:10.1029/145GM19, 2004.
- Lambeck, K., Rouby, H., Purcell, A., Sun, Y., and M., S.: Sea level and global ice volumes from the Last Glacial Maximum to the Holocene, *PNAS*, 111 (43), 15 296–15 303, doi:10.1073/pnas.1411762111, 2014.
- Lambert, F., Kug, J.-S., Park, R. J., Mahowald, N., Winckler, G., Abe-Ouchi, A., O'ishi, R., Takemura, T., and Lee, J.-H.: The role of  
10 mineral-dust aerosols in polar temperature amplification, *Nature Climate Change*, 3, 487–491, doi:10.1038/nclimate1785, 2013.
- Lambert, F., Tagliabue, A., Shaffer, G., Lamy, F., Winckler, G., Farias, L., Gallardo, L., and De Pol-Holz, R.: Dust fluxes and iron fertilization in Holocene and Last Glacial Maximum climates, *Geophysical Research Letters*, 42, 6014–6023, doi:10.1002/2015GL064250, 2015.
- Lamy, F., Gersonde, R., Winckler, G., Esper, O., Jaeschke, A., Kuhn, G., Ullermann, J., Martinez-Garcia, A., Lambert, F., and Kilian, R.:  
15 Increased Dust Deposition in the Pacific Southern Ocean During Glacial Periods, *Science*, 343, 403–407, doi:10.1126/science.1245424, 2014.
- Lüthi, D., Le Floch, M., Bereiter, B., Blunier, T., Barnola, J. M., Siegenthaler, U., Raynaud, D., Jouzel, J., Fischer, H., Kawamura, K., and Stocker, T. F.: High-resolution carbon dioxide concentration record 650,000–800,000 years before present, *Nature*, 453, 379–382, doi:10.1038/nature06949, 2008.
- Maher, B. A., Prospero, J. M., Mackie, D., Gaiero, D., Hesse, P., and Balkanski, Y.: Global connections between aeolian dust,  
20 climate and ocean biogeochemistry at the present day and at the last glacial maximum, *Earth-Science Reviews*, 99, 61–97, doi:10.1016/j.earscirev.2009.12.001, 2010.
- Mahowald, N., Kohfeld, K. E., Hansson, M., Balkanski, Y., Harrison, S. P., Prentice, I. C., Schulz, M., and Rodhe, H.: Dust sources and deposition during the last glacial maximum and current climate: A comparison of model results with paleodata from ice cores and marine sediments, *Journal of Geophysical Research*, 104 (D13), 15 895–15 916, doi:10.1029/1999JD900084, 1999.
- 25 Mahowald, N., Yoshioka, M., Collins, W., Conley, A., Fillmore, D., and Coleman, D.: Climate response and radiative forcing from mineral aerosols during the glacial maximum, pre-industrial, current and doubled-carbon dioxide climates, *Geophysical Research Letters*, 33, L20 705, doi:10.1029/2006GL026126, 2006a.
- Mahowald, N. M., Muhs, D. R., Levis, S., Rasch, P. J., Yoshioka, M., Zender, C. S., and Luo, C.: Change in atmospheric mineral aerosols in response to climate: Last glacial period, preindustrial, modern, and doubled carbon dioxide climates, *Journal of Geophysical Research*,  
30 111, D10 202, doi:10.1029/2005JD006653, 2006b.
- Mariotti, V., Paillard, D., Roche, D. M., Bouttes, N., and Bopp, L.: Simulated Last Glacial Maximum  $\Delta^{14}C_{atm}$  and the deep glacial ocean carbon reservoir, *Radiocarbon*, 55, 1595–1602, doi:10.2458/azu\_js\_rc.55.16295, 2013.
- Mariotti, V., Paillard, D., Bopp, L., Roche, D. M., and Bouttes, N.: A coupled model for carbon and radiocarbon evolution during the last deglaciation, *Radiocarbon, Geophysical Research Letters*, 1306–1313, doi:10.1002/2015GL067489, 2016.
- 35 Martin, J. H., Gordon, R. M., and Fitzwater, S. E.: Iron in Antarctic waters, *Nature*, 345, 156–158, doi:10.1038/345156a0, 1990.
- Martínez-García, A. M., Sigman, D. M., Ren, H., Anderson, R. F., Straub, M., Hodell, D. A., Jaccard, S. L., Eglinton, T. I., and Haug, G. H.: Iron Fertilization of the Subantarctic Ocean During the Last Ice Age, *Science*, 343, 1347–1350, doi:10.1126/science.1246848, 2014.
- Matney, M.: On the Probability of Random Debris Reentry Occuring on Land or Water, *Orbital Debris Quaterly News*, 16(1), 5, 2012.

- Monnin, E., Indermühle, A., Daellenbach, A., Flueckiger, J., Stauffer, B., Stocker, T. F., Raynaud, D., and Barnola, J.-M.: Atmospheric CO<sub>2</sub> concentrations over the Last Glacial Termination, *Science*, 291, 112–114, doi:10.1126/science.291.5501.112, 2001.
- Muscheler, R., Beer, J., Wagner, G., Laj, C., Kissel, C., Raisbeck, G. M., Yiou, F., and Kubik, P. W.: Changes in the carbon cycle during the last deglaciation as indicated by the comparison of <sup>10</sup>Be and <sup>14</sup>C records, *Earth and Planetary Science Letters*, 219, 325–340, doi:10.1016/S0012-821X(03)00722-2, 2004.
- Okazaki, Y., Timmermann, A., Menviel, L., Harada, N., Abe-Ouchi, A., Chikamoto, M. O., Mouchet, A., and Asahi, H.: Deepwater Formation in the North Pacific During the Last Glacial Termination, *Science*, 329, 200–204, doi:10.1126/science.1190612, 2010.
- Peltier, W. R.: Global Glacial Isostasy and the Surface of the Ice-Age Earth: The ICE-5G (VM2) Model and GRACE, *Annual Review of Earth and Planetary Sciences*, 32, 111–149, doi:10.1146/annurev.earth.32.082503.144359, 2004.
- Peng, C. H., Guiot, J., and van Campo, E.: Estimating changes in terrestrial vegetation and carbon storage: Using paleoecological data and models, *Quaternary Science Reviews*, 17, 719–735, doi:10.1016/S0277-3791(97)00045-0, 1998.
- Prentice, K. C. and Fung, I. Y.: The sensitivity of terrestrial carbon storage to climate change, *Nature*, 346, 48–51, doi:10.1038/346048a0, 1990.
- Prentice, K. C., Harrison, S. P., and Bartlein, P. J.: Global vegetation and terrestrial carbon cycle changes after the last ice age, *Nature*, 189, 988–998, doi:10.1111/j.1469-8137.2010.03620.x, 2011.
- Reimer, P. J., Baillie, M. G. L., Bard, E., Bayliss, A., Beck, J. W., Blackwell, P. G., Bronk Ramsey, C., Buck, C. E., Burr, G. S., Edwards, R. L., Friedrich, M., Grootes, P. M., Guilderson, T. P., Hajdas, I., Heaton, T. J., Hogg, A. G., Hughen, K. A., Kaiser, K. F., Kromer, B., McCormac, F. G., Manning, S. W., Reimer, R. W., Richards, D. A., Southon, J. R., Talamo, S., Turney, C. S. M., van der Plicht, J., and Weyhenmeyer, C. E.: INTCAL09 and MARINE09 radiocarbon age calibration curves, 0-50,000 years cal BP, *Radiocarbon*, 51, Nr. 4, 1111–1150, 2009.
- Reimer, P. J., Bard, E., Bayliss, A., Beck, J. W., Blackwell, P. G., Ramsey, C. B., Buck, C. E., Cheng, H., Edwards, R. L., Friedrich, M., Grootes, P. M., Guilderson, T. P., Hafliðason, H., Hajdas, I., Hatté, C., Heaton, T. J., Hoffmann, D. L., Hogg, A. G., Hughen, K. A., Kaiser, K. F., Kromer, B., Manning, S. W., Niu, M., Reimer, R. W., Richards, D. A., Scott, E. M., Southon, J. R., Staff, R. A., Turney, C. S. M., and van der Plicht, J.: INTCAL13 and MARINE13 radiocarbon age calibration curves 0–50,000 years cal BP, *Radiocarbon*, 55, Nr. 4, 1869–1887, doi:10.2458/azu\_js\_rc.55.16947, 2013.
- Rose, K. A., Sikes, E. L., Guilderson, T. P., Shane, P., Hill, T. M., Zahn, R., and Spero, H. J.: Upper-ocean-to-atmosphere radiocarbon offsets imply fast deglacial carbon dioxide release, *Nature*, 466(7310), 1092–1097, doi:10.1038/nature09288, 2010.
- Saugier, B., Roy, J., and Mooney, H. A.: 23 - Estimations of global terrestrial productivity: converging toward a single number, *Terrestrial global productivity: past, present and future*, pp. 543–557, doi:10.1016/B978-012505290-0/50024-7, 2001.
- Schaefer, K., Zhang, T., Bruhwiler, T., and Barrett, A. P.: Amount and timing of permafrost carbon release in response to climate warming, *Tellus*, 63B, 165–180, doi:10.1111/j.1600-0889.2011.00527.x, 2011.
- Schmitt, J., Schneider, R., Elsig, J., Leuenberger, D., Lourdantou, A., Chappellaz, J., Köhler, Joos, F., Stocker, T. F., Leuenberger, M., and Fischer, H.: Carbon Isotope Constraints on the Deglacial CO<sub>2</sub> Rise from Ice Cores, *Science*, 336, 710–714, doi:10.1126/science.1217161, 2012.
- Schmittner, A., Urban, N. M., Shakun, J. D., Mahowald, N. M., Clark, P. U., Bartlein, P. J., Mix, A. C., and Rosell-Melé, A.: Climate Sensitivity Estimated from Temperature Reconstructions of the Last Glacial Maximum, *Science*, 334, 1385–1388, doi:10.1126/science.1203513, 2011.

- Schneider von Deimling, T., Ganopolski, A., Held, H., and Rahmstorf, S.: How cold was the Last Glacial Maximum?, *Geophysical Research Letters*, 33, L14 709, doi:10.1029/2006GL026484, 2006.
- Schuur, E. A. G., Bockheim, J., Canadell, J. G., Euskirchen, E., Field, C. B., Goryachkin, S. V., Hagemann, S., Kuhry, P., Laffleur, P. M., Lee, H., Mazhitova, G., Nelson, F. E., Rinke, A., Romanovsky, V. E., Shiklomanov, N., Tarnocai, C., Venevsky, S., Vogel, J. G., and Zimov, S. A.: Vulnerability of Permafrost Carbon to Climate Change: Implications for the Global Carbon Cycle, *Bioscience*, 58, 701–714, doi:10.1641/B580807, 2008.
- Schuur, E. A. G., McGuire, A. D., Schädel, C., Grosse, G., Harden, J. W., Hayes, D. J., Hugelius, G., Koven, C. D., Kuhry, P., Lawrence, D. M., Lawrence, D. M., Natali, S. M., Olefeldt, D., Romanovsky, V. E., Schaefer, K., Turetsky, M. R., Treat, C. C., and Vonk, J. E.: Climate change and the permafrost carbon feedback, *Nature*, 520, 171–179, doi:10.1038/nature14338, 2015.
- Shaffer, G.: Biogeochemical cycling in the global ocean: 2. New production, Redfield ratios, and remineralization in the organic pump, *Journal of Geophysical Research*, 101, 3723–3745, doi:10.1029/95JC03373, 1996.
- Shaffer, G.: Long-term effectiveness and consequences of carbon dioxide sequestration, *Nature Geoscience*, 3, 464–467, doi:10.1038/NGEO896, 2010.
- Shaffer, G. and Sarmiento, J. L.: Biogeochemical cycling in the global ocean: 1. A new analytical model with continuous vertical resolution and high latitude dynamics, *Journal of Geophysical Research*, 100, 2659–2672, doi:10.1029/94JC01167, 1995.
- Shaffer, G., Malskær Olsen, S., and Pepke Pedersen, J.: Presentation, calibration and validation of the low-order, DCESS Earth System Model (Version 1), *Geoscientific Model Development*, 1, 17–51, doi:10.5194/gmd-1-17-2008, 2008.
- Shaffer, G., Olsen, S. M., and Pedersen, O. P.: Long-term ocean oxygen depletion in response to carbon dioxide emissions from fossil fuels, *Nature Geoscience*, 2, 105–109, doi:10.1038/NGEO420, 2009.
- Shakun, J., Clark, P. U., He, F., Marcott, S. A., Mix, A. C., Liu, Z. Y., Otto-Bliesner, B., Schmittner, A., and Bard, E.: Global warming preceded by increasing carbon dioxide concentrations during the last deglaciation, *Nature*, 484, 49–54, doi:10.1038/nature10915, 2012.
- Sigman, D. M. and Boyle, E. A.: Glacial/interglacial variations in atmospheric carbon dioxide, *Nature*, 407, 859–869, doi:10.1038/35038000, 2000.
- Sigman, D. M., Hain, M. P., and Haug, G. H.: The polar ocean and glacial cycles in atmospheric CO<sub>2</sub> concentration, *Nature*, 466, 47–55, doi:10.1038/nature09149, 2010.
- Sterner, R. W. and Elser, J. J.: *Ecological Stoichiometry: The Biology of Elements from Molecules to the Biosphere*, vol. 25(9), Princeton University Press, doi:10.1093/plankt/25.9.1183, 2002.
- Toggweiler, J. R. and Russel, J.: Ocean circulation in a warming climate, *Nature*, 451, 286–288, doi:10.1038/nature06590, 2008.
- Waelbroeck, C., Labeyrie, L., Michel, E., Duplessy, J. C., McManus, J. F., Lambeck, K., Balbon, E., and Labracherie, M.: Sea-level and deep water temperature changes derived from benthic foraminifera isotopic records, *Quaternary Science Reviews*, 21, 295–305, doi:10.1016/S0277-3791(01)00101-9, 2002.
- Watson, A. J. and Naveira Garabato, A. C.: The role of Southern Ocean mixing and upwelling in glacial-interglacial atmospheric CO<sub>2</sub> change, *Tellus*, 58B, 73–87, doi:10.1111/j.1600-0889.2005.00167.x, 2006.
- Zech, R.: A permafrost glacial hypothesis - Permafrost carbon might help explaining the Pleistocene ice ages, *Quaternary Science Journal*, 61(1), 84–92, doi:10.3285/eg.61.1.07, 2012.
- Zheng, D., Prince, S., and Wright, R.: Terrestrial net primary production estimates for 0.5 grid cells from field observations - a contribution to global biogeochemical modeling, *Global Change Biology*, 9, 46–64, doi:10.1046/j.1365-2486.2003.00534.x, 2003.

- Zickfeld, K., Eby, M., Weaver, A. J., Alexander, K., Crespin, E., Edwards, N. R., Eliseev, A. V., Feulner, G., Fichefet, T., Forest, C. E., Friedlingstein, P., Goosse, H., Holden, P. B., Joos, F., Kawamiya, M., Kicklighter, D., Kienert, H., Matsumoto, K., Mokhov, I. I., Monier, E., Olsen, S. M., Pedersen, J. O. P., Perrette, M., Philippon-Berthier, G., Ridgwell, A., Schlosser, A., Schneider Von Deimling, T., Shaffer, G., Sokolov, A., Spahni, R., Steinacher, M., Tachiiri, K., Tokos, K. S., Yoshimori, M., Zeng, N., and Zhao, F.: Long-term climate change commitment and reversibility: An EMIC intercomparison, *Journal of Climate*, 26, 5782–5809, doi:10.1175/JCLI-D-12-00584.1, 2013.
- 5 Zimov, N. S., Zimov, S. A., Zimova, A. E., Zimova, G. M., Chuprynin, V. I., and Chappin III, F. S.: Carbon storage in permafrost and soils of the mammoth tundra-steppe biome: Role in the global carbon budget, *Geophysical Research Letters*, 36, L02502, doi:10.1029/2008GL036332, 2009.

## ***Interactive comment on “An improved land biosphere module for use in reduced complexity Earth System Models with application to the last glacial termination” by Roland Eichinger et al.***

**Roland Eichinger et al.**

roland.eichinger@dlr.de

Received and published: 17 April 2017

### **Reply to:**

**SC1: 'Executive Editor Comment on "An improved land biosphere module for use in reduced complexity Earth System Models with application to the last glacial termination"', Astrid Kerkweg, 20 Jan 2017**

Dear authors, in my role as Executive editor of GMD, I would like to bring to your attention our Editorial version 1.1: <http://www.geosci-model-dev.net/8/3487/2015/gmd-8-3487-2015.html> This highlights some requirements of papers published in GMD, which is also available on the GMD website in the 'Manuscript Types' section: [http://www.geoscientific-model-development.net/submission/manuscript\\_types.html](http://www.geoscientific-model-development.net/submission/manuscript_types.html)

C1

In particular, please note that for your paper, the following requirements have not been met in the Discussions paper:

- "The main paper must give the model name and version number (or other unique identifier) in the title."

In order to simplify reference to your developments, please add a model name (and/or its acronym) and a version number in the title of your article in your revised submission to GMD.

Yours,  
Astrid Kerkweg

Dear Astrid Kerkweg,  
thank you for your comment. To address this we have now modified our title to read: "An improved land biosphere module for use in the DCESS Earth System Model (Version 1.1) with application to the last glacial termination"

---

Interactive comment on Geosci. Model Dev. Discuss., doi:10.5194/gmd-2016-306, 2017.

## ***Interactive comment on “An improved land biosphere module for use in reduced complexity Earth System Models with application to the last glacial termination” by Roland Eichinger et al.***

**Roland Eichinger et al.**

roland.eichinger@dlr.de

Received and published: 17 April 2017

### **Reply to:**

**Interactive comment on “An improved land biosphere module for use in reduced complexity Earth System Models with application to the last glacial termination“ by Roland Eichinger et al. from K. Crichton**

*Dear K. Crichton,*

*thank you for your comment. Please find our answers (in blue) to your comments (in black) below:*

C1

The study presents developments of the DCESS earth system model, for vegetation zones and for a permafrost carbon pool. They present some validation for the vegetation zones, and then go on to perform and discuss the simulation of the last glacial termination. I focus on the permafrost module here.

The amount of carbon stored in the area defined as permafrost in the model is 30kg/m<sup>2</sup>, an approximation from present-day near surface soil organic carbon data in Schuur et al 2015. The approach to define where is the permafrost, is to use the latitude  $L_{snow}$  (or  $L_{ice}$ , whichever is lower) at the 0degC global temperature (page 9 line 6: is this a typo? Do you mean  $L_{snow}$  is at the 0degC latitude? Perhaps this needs to be re-written).

To clarify we modified this text to read "During interglacials when ice sheets retreat poleward, the poleward boundary of this zone is taken to be the equatorward extent of permafrost. For simplicity we assume that this extent is defined by  $L_{snow}$ , the latitude of 0°C global mean temperature".

Whilst this would indeed create a dynamic pool of carbon sensitive to changes in the area of  $L_{snow}/ice$ , I am not convinced that this is a good representation of permafrost-carbon. If the concentration in this pool is fixed at 30kg/m<sup>2</sup>, then it cannot be properly taking account of the long time-to-equilibrium that would be seen in a permafrost-like carbon pool. Low accumulation and low decay rates means that the rate of change of area becomes important for soil carbon content. This is true for both release from "thawed" (i.e. no longer in  $L_{ice}/snow$ ) or newly permafrost (i.e. new  $L_{ice}/snow$ ) areas. They assume that this 30kg/m<sup>2</sup> is instantaneous for new areas, and is instantly released in thawed areas (is this the case in the model?). As such it is entirely dependent on the parametrisation of  $L_{snow}$  (and not soil carbon dynamics or decay rates). The mean value of 30kg/m<sup>2</sup> also does not take account of the true spatial heterogeneity of carbon content in permafrost soils. For example, some areas which underlay

C2

peatlands contain on the order of 100kg/m<sup>2</sup>+ organic carbon contents, and others far less than 30kg/m<sup>2</sup>. The spatial location of higher or lower-than-mean carbon content soils would make a big difference to carbon release rates. However, this is not possible to treat in this model (due to how it is set up) but should be mentioned.

I understand that this is a reduced complexity model, but it is important to incorporate accumulation and decay rates into a permafrost carbon pool model. This is especially true if the aim is to consider changing climates. At least this needs to be discussed in the text. See Zimov et al 2009 for example of the dynamic response of a permafrost-carbon model soil.

In the simplified context of the DCESS model, mean values and zonal boundaries characterise each of our three new vegetation zones and for consistency this approach was extended to our treatment of permafrost. As shown in Zimov et al. 2009, carbon release rates from permafrost for warming are rapid with time scales on the order of 100 years. Such time scales are comparable to those of extra-terrestrial forest reoccupation of areas freed from permafrost, a process that we also take to be “instantaneous” in the model. Thus there is also internal consistency in this point. On the other hand, carbon buildup in permafrost during cooling is a much slower process (Zimov et al. 2009) but we start our simulations from LGM conditions following 80,000 years of cooling. Thus we feel that our permafrost approach, although very simplified, should be able to capture the first order effects of permafrost on carbon cycling during deglaciation, as reported in our paper (but see also below). We will bring a discussion of these points more up front in our revision.

The authors say they tuned their model to a last glacial climate state, but this doesn't appear to include the amount of carbon on land. Although the total change of -408GtC from LGM to PI is in alignment with recent estimates, the starting point at LGM from 1800GtC (fig 1) is far lower than Ciais et al 2012 estimate (at 3640+-400GtC). The

C3

authors do state p18 line10 that their permafrost pool is underestimated (compared to Ciais et al 2012), but they need to quantify this. It makes a big difference to the LGM simulation discussion. For example, with a far larger LGM permafrost carbon pool it is unlikely that regrowth of the terrestrial biosphere would compensate permafrost thawing for land carbon flux. It would also pull their LGM-PI land carbon change out. This needs to be discussed.

Ms. Crichton is mistaken in stating that our LGM starting point for the amount of carbon on land is 1800 GtC. Rather this is our result for our new biosphere but does not include our estimate for permafrost. When that estimate is included (see Fig. 5) the total amount of carbon on land is about 2800 GtC, much larger but still somewhat low compared to the Ciais et al. 2012 estimate of 3640+-400GtC. To address this and our apparent underestimation of the permafrost pool we will carry out an additional simulation as a sensitivity study whereby we will use a doubled permafrost content, i.e. 60 kg of carbon per square meter. For this case our total amount of carbon on land will be about 3800 GtC, in good agreement with the Ciais et al. 2012 estimate. We will include the results of this new simulation in our Figs. 4 and 5.

The authors have put a lot of effort into improving the land biosphere module for vegetation zones, but the permafrost pool representation is less well developed and not well explored, and is not validated. They need to consider whether representing permafrost carbon dynamics in this way, assuming an instant equilibrium with climate of soil carbon, is appropriate (I think it's not). And if not, then to instead develop a separate permafrost model for use with DCESS.

As follows from what we wrote above, we will put more effort into explaining, exploring and validating our treatment of permafrost.

C4

Zimov, N. S., et al. "Carbon storage in permafrost and soils of the mammoth tundra-steppe biome: Role in the global carbon budget." *Geophysical Research Letters* 36.2 (2009).

---

Interactive comment on *Geosci. Model Dev. Discuss.*, doi:10.5194/gmd-2016-306, 2017.

## ***Interactive comment on “An improved land biosphere module for use in reduced complexity Earth System Models with application to the last glacial termination” by Roland Eichinger et al.***

**Roland Eichinger et al.**

roland.eichinger@dlr.de

Received and published: 17 April 2017

### **Reply to:**

**Interactive comment on An improved land biosphere module for use in reduced complexity Earth System Models with application to the last glacial termination by Roland Eichinger et al. from Anonymous Referee #1**

*Dear Anonymous Referee #1,*

*thank you very much for your comments and suggestions. Please find our answers (in blue) to your comments (in black) below:*

C1

### General comments

The paper presents a new terrestrial carbon cycle module within a the DCESS Earth System Model. Specifically, the authors expand the model, by accounting 3 vegetation zones, that can expand and contract, depending on global mean temperatures. The authors show, that the inclusion of these zones indeed creates a vastly different total vegetation carbon pool for glacial/interglacial transitions. They then couple the model with ocean and atmosphere content to evaluate the evolution of DELTA 14CO<sub>2</sub> delta 13CO<sub>2</sub>, as well as CO<sub>2</sub> concentration in the atmosphere during the last deglaciation.

I appreciate the work showing that indeed expanding and shrinking of areas of plant growth does have a significant effect and can indeed cause differences in the overall response to global temperature change. However, the authors seem to be caught in a conundrum when applying their model to glacial-interglacial change. On the one hand, they try to discuss the degree with which the change in atmospheric carbon proxy can be reproduced by their model, but they have to deal with the result that these changes are mostly the imprint of ocean dynamics and ocean carbon cycle. As a result, there is much back and forth in the paper between discussing the terrestrial biosphere module and the entire model - leading to some confusion. Perhaps a way to remedy the whole thing is to organize the results from the DCESS without model improvement, talk about what how the transition is set up and carry out glacial-interglacial simulation in absence of a terrestrial module. Having this out of the way the focus can remain on the terrestrial system. Thus, first focus is glacial interglacial change with ocean/atmosphere boundary/initial conditions, and perhaps run a simulation without any vegetation change. In a next step one can then compare against this null model with the crude DCESS terrestrial module (no vegetation zones) against the improvement in the land model. The comparison may also not just discuss the outcome of carbon cycle and its impact on the prediction (and feedback) of

C2

temperature, but it could also include albedo effects due to the different biomes as well (and methane? - The authors mention also a wetland module at one point). The focus would then not be so much on the degree with which the DCESS model can reproduce CO<sub>2</sub>, but how the land parameterization affects DCESS dynamics.

We appreciate these suggestions and are now restructuring the paper to accommodate them, thereby putting focus squarely on the new vegetation model. As part of this we now will compare the following six simulations of the last glacial termination in one or two of our figures: Simulation 1 (S1)→a nul model with no vegetation change but all other prescribed forcings, S2→S1 but using the old DCESS veg model, S3→S1 with the new DCESS veg model but no veg albedo effects nor permafrost, S4→S3 but including new veg albedo; S5→S4 but including permafrost (30kgC/m<sup>2</sup>) and S6→S4 but including increased permafrost (60kgC/m<sup>2</sup>; see also answer to K. Crichton's comment). This creates the desired shift of focus towards the effects of the land parameterisation on DCESS model dynamics. The discussion section will be restructured accordingly.

It is important to note that the terrestrial biosphere likely gains carbon. Thus it works against the accumulation of CO<sub>2</sub> in the atmosphere. In a way, your model improvement makes the situation worse. I think the author should point that out more clearly (despite the fact that the paleoclimate community is very well aware of). It also shows an important conundrum in modeling: Namely, even if you improve a model (and you know it), the outcome gets worse - which does not mean your model took a turn to the worse. In fact, such work help to foster continued model development.

We will discuss these points in more detail in the paper. As the data show and our model simulates, the terrestrial biosphere by itself likely gains carbon across the last termination. However, as shown in our Fig. 5, when permafrost is included there is an overall carbon loss that will increase for our new simulation with enhanced permafrost.

C3

Overall, I think the development and application of an improved terrestrial module in a reduced complexity Earth System Model is a worthy endeavor. These types of model can offer great insight since they can easily be modified and interpretation is much more straightforward. I am sure the presentation can be modified that the paper achieves this goal by focusing on how the modification affect the overall Earth system dynamics.

Specific comments:

Is methane considered as radiative forcing (methane emissions from terrestrial systems are briefly mentioned)? Also, is there a specific climate sensitivity applied to the model?

Yes, methane is considered as radiative forcing. As described in Shaffer et al. (2008), our old land biosphere model was tuned to emit the methane required to balance atmospheric oxidation while achieving observed pre-industrial atmospheric methane concentrations. We have adopted this approach for our new land biosphere model too but we found that this simple extension of our earlier approach led to values for LGM methane considerably higher than observed in ice cores, about 500 ppb compared to 350 ppb. So we decided to use prescribed methane (and nitrous oxide) concentrations from ice core observations for our radiative forcing calculations for our last termination simulations. However, inspired by the reviewer's comment we are revisiting our methane calculations with the idea to only allow methane production in the "wet" vegetation zones (tropical or tropical/boreal). Depending on our new results we may then use simulated methane (rather than prescribed) for our radiative forcing in the simulations and then, of course, include a new short section describing our new

C4

methane approach.

In our simulations we use a climate sensitivity of 2.5°C for a pCO<sub>2</sub> doubling as was explained and motivated in section S6 of our Supplement.

One of the limitations of the Gerber et al., 2004 study was, that they did not incorporate ice sheet, nor did they calculate potential effects of a reduced sea level. In particular, the reduction of sea level caused an additional and significant storage of carbon because of the expansion of the land mass. This may be worthwhile discussing - see e.g. Joos et al., 2004 for applications with LPJ - against which the comparison here has been made.

In our work we do in fact include the ice sheet area effect, albeit in a simplified way. On the other hand we did not include possible effects of sea level change and associated land exposure. In Joos et al 2004, this effect was found to be considerably less important than the ice sheet area effect or the climate/CO<sub>2</sub> change effect. However, we will discuss this point as suggested.

It seems to me central parameters to glacial/interglacial change are lambda\_Q (the Q10 factor), and fCO<sub>2</sub> (the CO<sub>2</sub> fertilization factor). Would it be worthwhile to test the sensitivity of these in the DCESS outcomes?

These are of course central parameters in any land biosphere model but here we prefer not to go into sensitivity studies based around variations of these parameters. We feel that that would carry us too far afield. Furthermore, the values for the parameters we now use have proven to give comparable land biosphere results in recent intercomparison studies of past and future warming and pCO<sub>2</sub> change (Eby et al 2013, Climate

C5

of the Past; Zickfeld et al 2013, Journal of Climate). When we participated in these studies we found that the original DCESS model fertilisation factor (0.62; Shaffer et al, 2008) appeared to be too high. By reevaluation of this we arrived at a lower value (0.37) that we used in the 2013 studies and continue to use today.

Method section: Parts of it seems to be result: I believe the simplistic model behavior should be juxtaposed with the improvement in the model section. In particular figure 1 should not appear in the method section, but be actually part of the results.

We agree that the section of land biosphere albedo, including Fig. S1, should have been included in the main text and in the revision we will do so. As mentioned above, we will also do a sensitivity study of the effect of land biosphere albedo.

Equations 1 and 2: This is a 5th degree polynomial, is there a justification to use 5 degrees, can the extent not adequately represented by 3 degrees? I think it may be important to keep the number of parameters low in a reduced complexity Earth system model.

The answer to this requires a more in-depth description, both here and in our revision, of how we arrived at these curves. Our point of departure was the total tree cover frame of Fig. 4 of Gerber et al. 2004, Global Biogeochemical Cycles. On that frame we read off, at 2°C intervals from -10 to 10°C deviation from pre-industrial global mean temperature, the latitudes in the Northern Hemisphere of 50% tree cover both above and below the subtropical zone of lower tree cover. Each of these two sets of 11 points formed the basis for our curve fitting. We found that 5th order polynomials provided good fits to each of these sets whereas 3rd order polynomials did not, in particular for the tropical/grassland boundary. In our revised manuscript we will plot the individual

C6

"data" points in Figure 2.

Equations 14-18: It seems these equations do not balance the carbon flux e.g. 10/60 of the leaf loss is unaccounted for. Also I don't understand equation 18: the units seem to be off and I don't see where the 45/55 comes from: In my understanding equation 18 should be the sum of equations 14-17.

There is a mistake in Equation 16. The fraction just to the right of the equal sign should be 35/60 (not 25/60), explaining the imbalance pointed out by the reviewer, This is an error only in the written equation of the manuscript; the model code uses the correct equation. As stated in Shaffer et al, 2008, "...NPP is distributed between leaves and wood in the fixed ratio 35:25, all leaf loss goes to litter, wood loss is divided between litter and soil in the fixed ratio 20:5, litter loss is divided between the atmosphere (as CO<sub>2</sub>) and the soil in the fixed ratio 45:10. Soil loss is to the atmosphere as CO<sub>2</sub>...". This helps to explain the other fractions in equations 16 and 17. Unfortunately as pointed out by the reviewer, Equation 18 is in error as written down in the manuscript (but not in error in the corresponding model code equation). In the manuscript Equation 18 should read

$$F_{CO_2} = \sum_{i=1}^3 -NPP^i + \frac{45}{60}NPP_{PI}^i \cdot \lambda_Q^i \frac{M_D^i}{M_{D,PI}^i} + \frac{15}{60} \cdot NPP_{PI}^i \cdot \lambda_Q^i \frac{M_S^i}{M_{S,PI}^i}$$

As pointed out by the reviewer, Equation 18 should be the sum of equations 14-17. This was so in the model code and now is also the case in the manuscript equations. Furthermore, Equation 19 is now also being corrected in the same manner in the manuscript.

I have trouble understanding how you calculated permafrost release. There are 2 numbers, one considers a permafrost storage of 30 kg m<sup>-2</sup>, but what is the 0.33 kg

C7

m<sup>-2</sup>? And how is this number linked to the isotope ratio? This may be my limitation, but perhaps there are ways to clarify this.

The number 0.33kg·m<sup>-2</sup> (actually 0.329....) is the amount of <sup>13</sup>C needed to yield a δ<sup>13</sup>C of -24 in permafrost soil, given the assumption of a constant 30kg·m<sup>-2</sup> carbon in permafrost. It is calculated using Eq. S11 of the Supplement. For clarity we will include this information in the revised text.

Figure 6: It is not clear what the production rate is in the ALL\_TF simulation (red line).

The ALL\_TF simulation uses the production rate from Hain et al. (2014), as stated in the figure caption.

Discussion of transient simulations: A great deal of this discussion focuses on ocean carbon cycling, which is not surprising given that the ocean dominates the carbon cycle on this time scale. However, there is little support to the items raised in the paper. Where is it detailed out, how much each of the radiative forcing contributes to the temperature increase (dust etc.), and how this affect isotopic distributions. In some instances, it may be sufficient to point to the appropriate figure/text in the supplementary material, but perhaps it is also worthwhile considering additional plots. And again, I suggest some restructuring to better set apart the overall mechanisms of glacial/interglacial carbon cycling from the discussion of the improved vegetation dynamics.

Through the above described restructuring of the paper, the discussion of ocean carbon cycling is now put more into the background. Furthermore, we now clearly state where individual items raised in the discussion are supported, basically that is Figure

C8

S7 and Table S3. However, to maintain the focus of the paper on land carbon cycling, we refrain from adding more plots on these topics to the manuscript.

P9L23. Starting from “As is, ... “ until the end of paragraph, this seems to be misplaced.

We may not have made clear enough why we include this text here. The model land fraction in this latitude range of changing permafrost extent is important since we want a global permafrost estimate but work with a model that represents the Earth with one generic hemisphere. If the mean land fraction of North and South Hemisphere (in that latitude range) was very different from the model land fraction, some scaling for the permafrost effect would be required. We now underline the importance of this point by revising the paragraph to read:

Land area uniformly covers 25% of the globe from the equator to 70 degrees latitude in the one hemisphere, DCESS model. For our model last glacial termination, permafrost affects latitudes between 47° and around 54° (see Fig. S3 in the Supplement), and is estimated as a two hemisphere mean. Across these latitudes, the land fraction averaged over both hemispheres is around 30% (see e.g. Matney, 2012). Thus we did not feel it to be necessary to further scale the permafrost effect due to global mean land fraction.

P10L4: Please also state what the initial global temperature is (14 degree C?)

The initial global temperature is 15°C and is now included in the text.

P2L12: Check abbreviation for extratropical forest

C9

Corrected to EF in the text. Thanks again to the reviewer for careful reading of our manuscript.

---

Interactive comment on Geosci. Model Dev. Discuss., doi:10.5194/gmd-2016-306, 2017.

## ***Interactive comment on “An improved land biosphere module for use in reduced complexity Earth System Models with application to the last glacial termination” by Roland Eichinger et al.***

**Roland Eichinger et al.**

roland.eichinger@dlr.de

Received and published: 17 April 2017

### **Reply to:**

**Interactive comment on “An improved land biosphere module for use in reduced complexity Earth System Models with application to the last glacial termination” by Roland Eichinger et al. from Anonymous Referee #2**

*Dear Anonymous Referee #2,*

*thank you for your comments and suggestions. Please find our answers (in blue) to your comments (in black) below:*

C1

### General comments:

The authors present an improved land biosphere module which is then used in a reduced-complexity Earth system model to simulate the last glacial termination with a focus on carbon cycle changes. Although the processes causing the CO<sub>2</sub> rise during the last glacial termination are far from being understood and contributions to increase this understanding are highly welcome, I have some major concerns about this paper.

I'm not very convinced by the structure of the paper. The paper focuses on the description of an improved land biosphere component on the one side and on the coupled Earth system model response during the last glacial termination on the other side. Much of the changes in the global carbon cycle in the model during the last termination are due to changes in the ocean carbon cycle resulting mostly from prescribed transition functions. It is therefore not very clear what the message of the paper is supposed to be. Focusing only on the carbon cycle changes driven by the land and how the improvements to the land model affect the simulated land carbon response during deglaciation would probably result in a more straightforward message being delivered to the readers.

In the revised version, the paper is being restructured to put the focus squarely on carbon cycle changes driven by the land and how land model improvements affect carbon cycling during deglaciation. We now start the results and the discussion from an additional simulation with constant land biosphere, followed by the old and the new biosphere model transition simulations and the discussion on permafrost impact. Thereafter, the evaluation of the impacts of individual transition functions for the transient simulation starts. This creates a shift of focus towards the role of the land biosphere on

C2

climate and carbon cycling and the discussion of ocean carbon cycling is now moved more into the background. Please also see also our answers to reviewer 1.

The authors claim that they have improved the land model but the improvements are discussed only in a very qualitative manner. Several quantities could be compared with observed or reconstructed (also model-based) values, e.g. permafrost area (both present day and LGM) and permafrost carbon content (present day), NPP (LGM).

We do in fact compare our calculations for land and permafrost carbon storage change between pre-industrial and LGM to other estimates (Sections 2.4 and 3.2). In the revised version we are extending these comparisons to present day and LGM carbon stocks as well. For example, we now state that our total LGM amount of carbon on land is about 2800 GtC (land biosphere plus permafrost), which is somewhat low compared to the Ciais et al. 2012 estimate of  $3640 \pm 400$  GtC. We discuss how this can lead to an underestimation of the permafrost effect in the transition simulation and carry out an additional sensitivity simulation with a doubled concentration for permafrost carbon (also see our above response to K. Crichton on this).

A great advantage of a simple model over more complex models is the lower computational cost. This strength could be exploited to perform some parameter sensitivity analysis which would help to understand how robust the presented results are to changes in unconstrained parameter values. I'm a bit disappointed that this has not been done in the paper.

As discussed in our response to reviewer 1, we prefer to retain our values for central parameters like  $Q_{10}$  and  $f_{CO_2}$  since the values we use have proven to give comparable land biosphere results to those of other models in recent intercomparison studies of

C3

past and future warming and  $pCO_2$  change. Also as discussed above we are now doing additional sensitivity studies, for example using a doubled concentration for permafrost carbon.

It is questionable if a progress in understanding the role of land carbon changes during glacial termination can be attained by using the extremely simplified model described in this study for several reasons:

1) In the model, permafrost carbon reacts instantaneously to changes in the snow-ice line. This seems a quite crude parameterization and neglects the long time scales associated with permafrost carbon dynamics. The assumption of a uniform permafrost carbon concentration of 30 kgC/m<sup>2</sup> is not supported by observations which show large spatial variations in permafrost carbon over Siberia. At least a sensitivity analysis to this value would be appropriate.

For this see the detailed response to K. Crichton on DCESS model structure, very different time scales for uptake and release of permafrost carbon and consistency with the treatment of the land biosphere. Furthermore, as mentioned several times earlier, we will be carrying out an additional sensitivity simulation using a uniform permafrost carbon concentration of 60 kgC/m<sup>2</sup>.

2) The Northern Hemisphere ice sheet extent at LGM is strongly dependent on longitude, with the Laurentide ice sheet over North America extending as far south as 50°, while Siberia was ice-free. The implications of this asymmetry, which can not be considered in a zonally averaged model, should at least be discussed in the paper.

In fact the Laurentide Ice Sheet extended as far south as 38°N during the LGM. To

C4

account for this and the lack of an ice sheet in large parts of Siberia and within the constraints of our zonally-averaged model, we prescribed the southernmost ice sheet extent to be 47° and used ice sheet reconstructions to estimate a time series of ice sheet extent retreat (see Section 3.1). We feel that this is a meaningful approach and the best that can be done to be consistent with the degrees of complexity in the other model modules. We will supply some more discussion on this in the revision.

3) How the polynomial relations for the latitude of the borders between vegetation zones are derived from Fig. 4 in Gerber et al. (2004) is not very clear. Since this is supposed to be a technical paper, some more details could be given. On what quantity is the separation between vegetation zones based? What is the justification for using a 5-th order polynomial? Also, what is the zone north of the snowline considered to be?

The first two of these questions are dealt with in detail in a response to reviewer 1, including new additions to the revised manuscript. In our simplified approach the zone poleward of the snowline (0°C) is taken to be permafrost. In our revised version we will mention this up front in Section 2.1 to avoid confusion.

For the LGM cooling relative to preindustrial the IPCC gives a very likely range of 4-7°C cooling, while a value of 3.5°C is used in the model based on Shakun et al. 2012. This is only one example where a sensitivity analysis would be appropriate. I would expect the choice of global temperature at LGM to have a large impact on the simulated land carbon storage at LGM.

Recent estimates based on much improved temperature data have shown LGM cooling of 3.2 - 4°C (Shakun et al. 2012; Schmittner et al., 2011, Science; Annan and Hargreaves, 2013, Climate of the Past). Earlier studies based on much less data found

C5

considerably greater LGM global mean cooling (e. g. Schneider von Deimling et al., 2006; Geophysical Research Letters). Thus we feel that the choice of a 3.5°C LGM cooling is well motivated. Furthermore, our simulations use a modest climate sensitivity of 2.5°C based in part on the well-constrained LGM cooling we use (see Section S6 of our Supplement). Otherwise, our Fig. 1b provides a sensitivity analysis for our new land biosphere model like that proposed by the reviewer. The figure shows only a reduction in land biosphere carbon storage of about 50 GtC for a 5°C LGM cooling compared to a 3.5°C cooling. Furthermore, as shown in our Fig. 2, the model snowline does not extend equatorward of 47° for a 5°C cooling such that our prescribed ice sheet extent continues to form our equatorward permafrost extent. In the model this translates to no change in permafrost carbon storage for a 5°C LGM cooling compared to a 3.5°C cooling. Some of the above will be included in the revision.

Specific comments:

The last part of the last sentence on page 2 would fit into the abstract. I would suggest moving the discussion of Figure 1 (sentences on page 3, lines 25-27 and 31-34) to section 2.4.

These are good suggestions and are being adopted in the revision.

In the caption of Table 1, 'globally averaged for one hemisphere' should be replaced with e.g. 'integrated over one hemisphere'. (And why not give the global values instead of hemispheric values? That would make the values more easily interpretable.)

We also follow the reviewer's suggestion here and are providing global values in Table 1 in the revision. The table caption is being revised to read: Table 1. Pre-industrial

C6

distribution of carbon storage among model land carbon pools as well as model net primary production for the three vegetation zones (see Chapin et al., 2011, and citations therein).

Page 5, line 4: what do the authors mean by 'latitude of 0°C global mean temperature'?

In our model, a meridional temperature distribution in the atmosphere is obtained by fitting a second-order Lagrange polynomial to the atmospheric temperature of the low-mid latitude and high latitude boxes (see Shaffer et al, 2008). For clarification, in our revision we are modifying this text to read "During interglacials when ice sheets retreat poleward, the poleward boundary of this zone is taken to be the equatorward extent of permafrost. For simplicity we take this extent to be the latitude of our model equatorward snow cover extent,  $L_{\text{snow}}$ , defined by the latitude at which global mean atmospheric temperature is 0°C in our zonally-averaged model".

In section 2.1, first the separation of vegetation zones should be described and only afterwards Table 1 should be discussed. The total area of each vegetation zone should also be given together with the values of biomass reservoirs and NPP in Table 1.

We are also adopting these reviewer suggestions in our revision.

Page 9, line 4 and 7: 'BF' -> 'EF'

Thanks, done.

Page 12, line 3: 'agree well WITH other estimates'.

C7

This has now been corrected.

Page 12, lines 5: I can't see how the authors can say something about improvements in the 'timing' of carbon exchanges between land and atmosphere based on the results presented in the evaluation section

With the new vegetation scheme, a better quantitative description of the respective land biosphere pools is possible, including their individual reaction to temperature now calculated separately for each zone. As shown in Figure 3 for example, the TF zone vegetation reacts rapidly to temperature change since it is dominated by above-ground vegetation. Such differentiation was not possible with the old scheme and hence the timing of changes could not be represented as accurately as with the new scheme. We will try to make this clearer in the revised manuscript text.

---

Interactive comment on Geosci. Model Dev. Discuss., doi:10.5194/gmd-2016-306, 2017.

C8